Available online at www.sciencedirect.com
ScienceDirect
Coordination Chemistry Reviews 251 (2007) 203–221
COORDINATION CHEMISTRY REVIEWS
www.elsevier.com/locate/ccr

Review

Recent advances in the synthesis and properties of ferrocenes having an unsaturated backbone

Paromita Debroy, Sujit Roy *

Organometallics and Catalysis Laboratory, Chemistry Department, Indian Institute of Technology, Kharagpur 721302, India

Received 2 August 2005; accepted 1 July 2006
Available online 14 July 2006

Contents

Abstract

The design motif in ferrocene-based architectures plays an important role to secure the targeted chemical, electronic, opto-electronic, redox properties. One of such architectures includes motifs bearing an unsaturated backbone attached to one or both the cyclopentadienyl ring. This review focuses on the synthesis and properties of these special classes of ferrocenes having olefinic, and acetylenic and cumulenic backbones.

Keywords: Ferrocene; Unsaturation; Synthesis; Redox; Electronic; Opto-electronic

* Corresponding author. Tel.: +91 3222 283338; fax: +91 3222 282252.
E-mail address: sroy@chem.iitkgp.ernet.in (S. Roy).

0010-8545/$ – see front matter © 2006 Elsevier B.V. All rights reserved.
doi:10.1016/j.ccr.2006.07.001

1. Introduction

More than five decades after its discovery [1–4], ferrocene still evokes a great deal of research interest from scientists across the borders. Chiral and achiral ferrocenyl phosphines have been extensively used as ligands in organic synthesis and asymmetric catalysis for carbon–carbon, carbon–heteroatom coupling, carbonylation, hydroformylation, hydrogenation, olefin polymerization and cycloaddition [5–8]. The noteworthy application of ferrocenes also lies in other diverse areas such as molecular materials, charge-transfer complexes, photonics and liquid-crystals [5,9,10], in the field of supramolecular chemistry [11–13], as redox-sensors [14–18], as dendrimers and polymers [19–21], and in drug designing [22,23]. Undoubtedly, the design motif in ferrocene-based architectures plays the most important role to deliver the targeted property.

Linearly substituted ferrocenes having substitution at one or both Cp rings constitute a very broad sub-group of ferrocene architectures. The linear arm(s) may bear all carbon or heteroelements, heterocyclic rings, may be saturated, unsaturated or have an extended π-conjugation with the ferrocene nucleus. Four structural types may represent the majority of ferrocenes with linear open-arm motif according to whether the ferrocene nucleus is mono or disubstituted or whether the ferrocene acts as pillars to form "molecular clefts" (Chart 1).

Within the linear open-end motifs, those in which the ferrocene unit is appended with having unsaturated side-arms π-conjugated to the cyclopentadienyl ring, are of significant interest. Very broadly, these are of three types—olefinic, acetylenic and cumulenic (Chart 2). In the past one and half decade different research groups have created a range of these architectures with the sole aim to tune their chemical, electrochemical, spectroscopic, and opto-electronics properties. As a result, they have gained prominence as new generation molecular materials, π-conjugated multi-metallic systems and as redox-switchable receptors.

In this review, we focus on this special class of ferrocenes, and present a comparative assessment on recent advances in their synthesis and properties. In Section 2, we attempted to closely look into these systems under subcategories representing types of unsaturation in the side chain and to highlight selected examples in detail. Section 3 delineates the major routes to construct ferrocenes bearing ene-, yne- and cumulene motifs in a systematic manner. Finally, in Section 4, we have summarized their properties, and tried to analyze the question: '*Why π-extended conjugation to ferrocenyl platform?*'

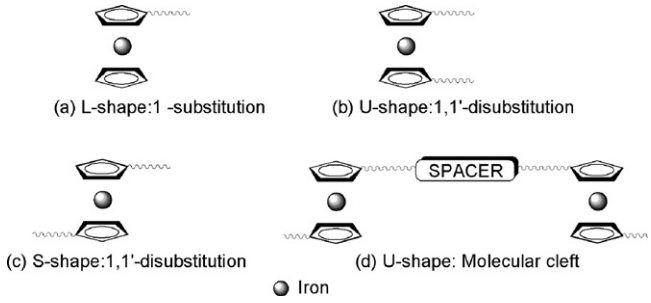

Chart 1. Linear structures of ferrocenes.

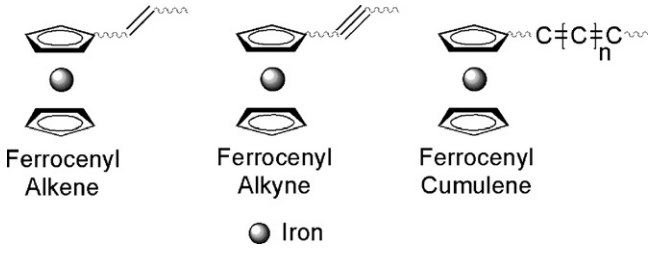

Chart 2. Types of ferrocenes with an unsaturated backbone.

2. Linear ferrocenes with open-end and unsaturated spacers

2.1. Ferrocenes with an olefinic backbone

Among the large number of reported ferrocenes bearing olefinic unsaturation at the side-arm, there lies an enormous amount of diversity depending on the number and nature of substituents on the unsaturated backbone. Broadly, they can be divided into four types:

I. Backbone having an olefinic spacer;
II. Backbone having a conjugated phenyl-ethenyl spacer;
III. Backbone having an olefinic spacer and ferrocene terminus at both ends;
IV. Two- and three-dimensional poly(ferrocenes) connected via arms having an olefinic spacer.

2.1.1. Type I: backbone having an olefinic spacer

The first type includes the ethenyl-containing ferrocene compounds (Chart 3). Simplest example of this is the vinyl ferrocene. However, its easy susceptibility towards polymerization has perhaps prompted researchers to further modify the vinylic fragment. Substitution at the vinylic end with aromatic and heteroaromatic groups has led to many interesting compounds. Compound **1** (Ferrocifen) with two phenyl rings at the vinyl end is the organometallic analogue of Tamoxifen and is a promising candidate for bio-evaluation towards anti-tumor screening [23]. Replacing the aromatic rings by pyridyl units as in compound **2** generates the modified Fc-anchored N-donor ligand, which shows strong affinity towards platinum(II). Interestingly, the redox property of the Pt(II) complex can be controlled by changing the degree of conjugation between the ferrocene center and the dipyridyl unit, indicating through bond communication between the two metal centers [24]. Compound **3** represents an aza-analogue of vinyl ferrocene having an extended conjugation between the dipyridyl unit and the Cp moiety [25]. The vinyl end has also been subjected to π-extension. Simple substitution with a –C=C– or a –C≡C– moiety leads to the ferrocenyl butadiene **4** and the ferrocenyl enyne **5** derivatives, respectively [26]. Further extension of the olefinic backbone leading to a rigid

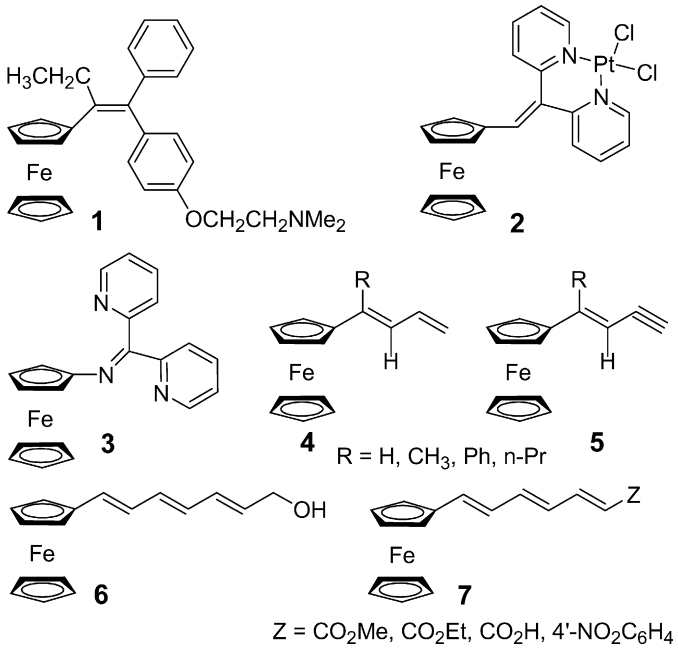

Chart 3. Types of ferrocenes with a modified vinylic backbone.

unsaturated triene chain conjugated to the ferrocene platform as in **6** and **7** has also been achieved [27,28]. In this connection, recent reports of soluble poly(ferrocenyl) acetylenes are noteworthy [29].

2.1.2. Type II: backbone having a conjugated phenyl-ethenyl spacer

The second type pertains to compounds containing electron-accepting groups linked to the ferrocene by a conjugated phenyl-ethenyl spacer. A few representative examples are summarized in Chart 4. The impetus for designing such molecular motifs comes from the fact that ferrocene is a moderate electron-donating fragment, so that connection to an electron-accepting moiety through a conjugated spacer further enhances opto-electronic communication leading to interesting non-linear optical properties. Indeed **8** with a *para*-nitrophenyl electron-accepting moiety is found to have a powder second harmonic generation (SHG) efficiency 62 times that of urea and even larger values of SHG (200 times urea) have been reported for $[\mathbf{9}]^{+}[\mathrm{I}]^{-}$ [30].

Peris and other groups have achieved interesting structure variations by placing a wide variety of pendant electron-accepting substituents (nitro, nitrile, pyridine, oxazoline) to the phenyl-ethenyl spacer linked to the ferrocene fragment. These are represented in a general way by structure **10** [31,32]. By further coordinating the pyridine and the nitrile terminated ferrocene compounds to metal carbonyl fragments $M(CO)_5$ (M = Cr, Mo, W) Peris has developed a wide class of heterometallic push–pull complexes, as shown in the generalized structure **11**.

Molecule **12** is a representative example of ene-conjugated ferrocenes having a tailor-made binding site for guest recognition [33]. The ene-conjugation in such structural motifs aid in facile electronic communication between the binding site and the redox site. Thus, compound **12** having a crown-ether binding site acts as a redox-switchable receptor towards the recognition of groups IA and IIA guest cations.

2.1.3. Type III: backbone having an olefinic spacer and ferrocene terminus at both ends

The third structural motif in the class is generated by linking olefinic chain/fragment between two ferrocene units (compounds **13**–**14**); bis(ferrocenyl)-ethylene **13** being the simplest molecule in this group (Chart 5) [34,31]. Besides an olefinic spacer, many examples containing different aromatic and heteroaromatic rings for conjugation between the ferrocene units are also reported in the last few years; selected examples are shown in Chart 5 (compounds **15**–**17**) [35–37]. Biferrocenes of this type can behave as potential molecular wires with effective intermetallic electronic communication. For example, in **15** ($n = 5$) the metal-to-metal distance, and the effective conjugation pathway are 40 and 51 Å respectively.

2.1.4. Type IV: poly(ferrocenes) connected via arms having an olefinic spacer

The fourth motif comprises of the two- or three-dimensional poly(ferrocene) systems diverging from varying core molecules via ethenyl or phenyl-ethenyl spacers (for example, compounds **18**–**22** in Chart 6) [38–42]. Tetraferrocenylethylene **18** is the

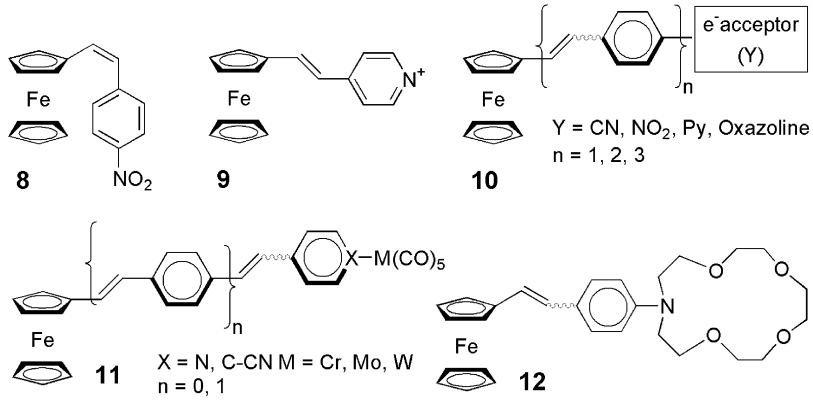

Chart 4. Types of ferrocenes with a modified phenyl-ethenyl spacer.

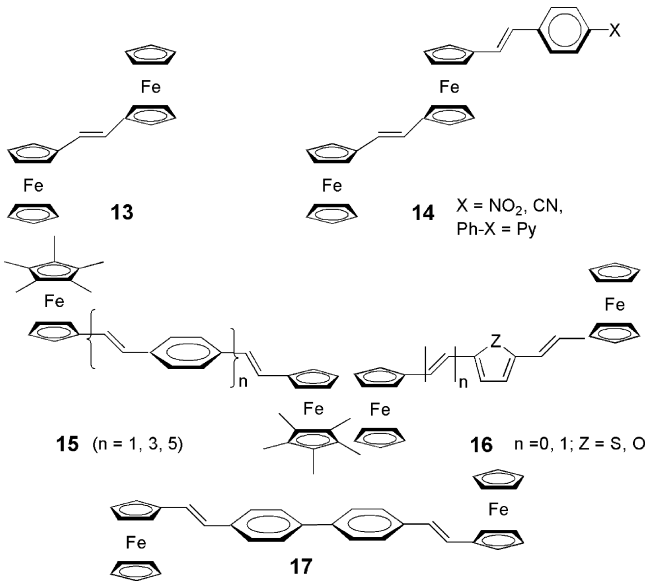

Chart 5. Ferrocenes linked through a vinyl unit.

simplest in this group with four ferrocene units linked by a single ethylene core and is one of the most distorted olefins known. This is prominent from its propeller shape with an elongated and twisted double bond. While both the star-shaped bi-dimensional ferrocene dendrimer **20** and the paracyclophane core containing dendrimer **21** bear conjugated vinyl arms, **22** is a novel dendritic structure in which the core of the dendrimer consists of a triphosphazene moiety and the arms bear imine conjugation.

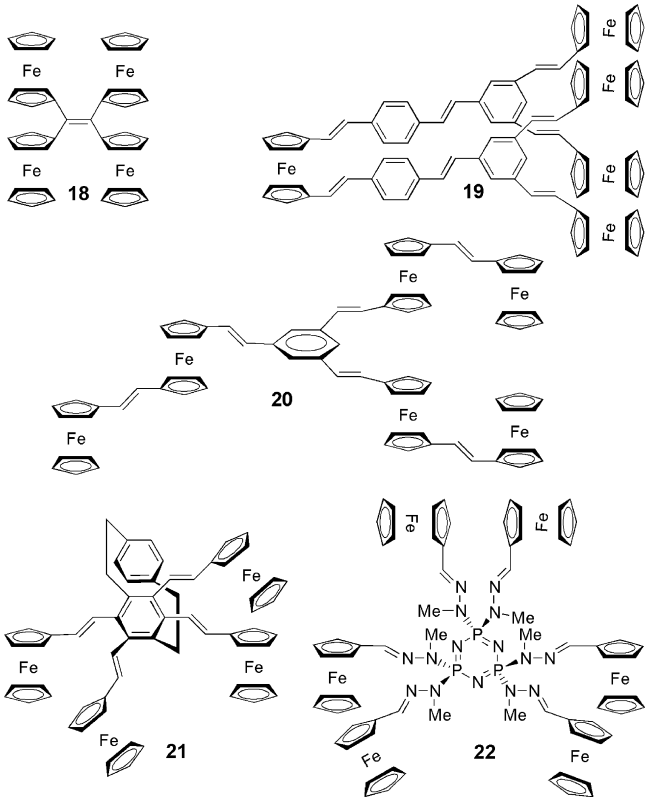

Chart 6. Ene-conjugated ferrocene dendrimers.

The impetus for developing these systems is perhaps the growing interest in organometallic dendrimers and polymers. Undoubtedly, the ferrocene dendrimers draw special attention because of their high degree of thermal and redox stability as well as well understood electrochemical properties. Additionally, the conjugative spacers enhance the electronic communication between the terminal redox centers.

2.2. Ferrocenes with an acetylenic backbone

π-Conjugated ferrocene systems having an acetylenic skeleton have become the design target of many research groups. Such motifs have potential applicability in the field of material sciences, in the study of metal–metal interaction and electronic communication as in molecular wires. Two general types can be used to represent the ferrocenyl acetylenes:

I. Backbone having an ethynyl spacer;
II. Di- and tri-ferrocenes connected via arms having an acetylenic spacer.

2.2.1. Type I: backbone having an ethynyl spacer

The first type includes those examples where the ethynyl fragment is linked directly or indirectly to the ferrocene platform. The acetylenic terminus is often capped with aromatic, heteroaromatic and metallic substituents to harness desired optical, opto-electronic and material properties (Chart 7). Structure **23** shows a general representation where aryl and various substituted aryls have been placed in conjugation with the acetylenic unit [43–45]. Interestingly, placing a benzonitrile group has provided an added opportunity for further co-ordination with a $Pd(PPh_3)_2$ unit, giving rise to the trimetallic species **24**. One-dimensional polymers have been synthesized by placing oligothiophene and pyridine groups on the acetylene skeleton, and subsequent metal co-ordination providing mixed valence bimetallic fragments **25** and **26** that are potential candidates for molecular wires [46,47]. Indeed, an insight into the delocalization along the conjugated backbone can be obtained from the analysis of their strong ligand to metal charge-transfer bands. Compound **27** is a much more extended phenyl-ethynyl congener linked to a metallic end-cap via a fluoren-9-one spacer [48].

As in the case of ferrocenes with an olefinic spacer, ferrocenyl acetylenes capped with electron-accepting groups result in non-linear optical properties. Compound **28** is an example having a tricarbonyl(cyclohexadienyl) iron(1+) unit acting as the cap [49]. The interesting aspect of the molecule is that, not only does it show a high hyperpolarisability (β) value of 100×10^{-30} esu (in comparison to $\beta = 16.9 \times 10^{-30}$ esu for 4-nitroaniline), but also have the advantage of a chiral electron-accepting organometallic end-group.

2.2.2. Type II: backbone having an acetylenic spacer and ferrocene terminus

The second type of motif consists of two or more ferrocene units linked by extended acetylene fragments and organic and inorganic spacers. By tuning the size and shape of the spacers,

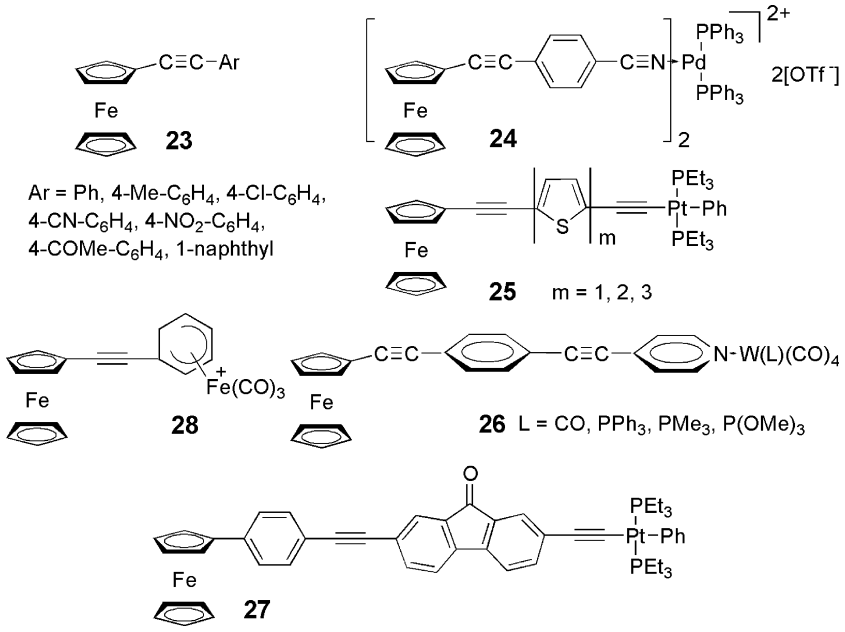

Chart 7. Ferrocenes with an ethynyl spacer.

elegant molecular architectures with possible electronic communication between the metal centers along the conjugated backbone have been achieved. A few representative examples are shown in Chart 8. Structure **29** is a general representation of ferrocenyl end-capped acetylide complexes with different types of aromatic and heteroaromatic spacers (Ar) [50–52]. It is to be noted that the presence of an acridine spacer leads to successful ethynylferrocenyl dyads. In order to study the effect of electron-donating and electron-deficient groups on the terminal ferrocenyl moieties, Wong et al. have designed a series of ferrocenyl end-capped derivatives **30** by varying the number of acetylenic units and the nature of the fluorene spacer [53]. Electrochemical studies reveal that the half-wave potential of the terminal ferrocene becomes more anodic upon increasing the number of ethynyl units and on changing the 9-substituent of the central fluorene ring from electron-donating alkyl or ferrocenyl group to an electron-deficient oxo group.

Compound **31** having three ferrocene termini connected by the triethynylbenzene core is noteworthy as it may be viewed as a potential precursor for the production of metal–aromatic polyyne network [54].

Besides organic spacers, many examples containing different metal bridging groups between the ferrocene units are reported in recent years, compound **32** being one such case (Chart 9) [55]. Particularly, notable is the dependence of the electronic communication between the two ferrocenyl units on the ancillary ligand at the ruthenium center lying in conjugation to the extended acetylide chain. The interaction is enhanced when the ligand is electron-donating, and reduced when it is electron-withdrawing.

2.3. Ferrocenes with a cumulenic backbone

The incorporation of quasi-one-dimensional allene and cumulene framework onto the ferrocenyl scaffold can also produce linear π-conjugated and delocalized ferrocene architectures. Bildstein has developed a series of allene and cumulene

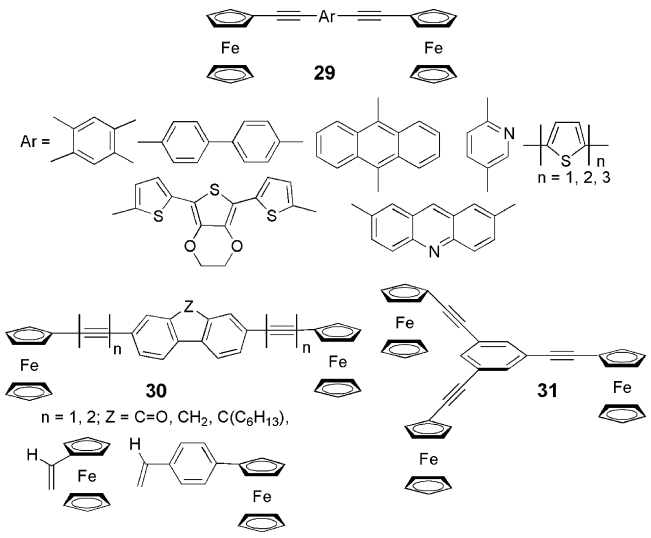

Chart 8. Ferrocenes linked through an acetylenic unit.

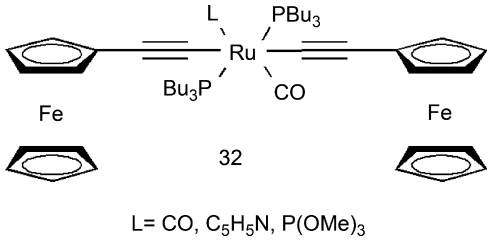

Chart 9. Ferrocenes linked by metal spacer and an acetylenic unit.

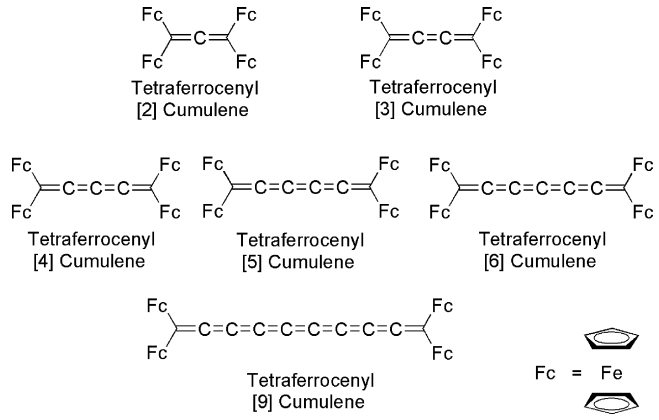

Chart 10. Overview of cumulenes with ferrocenyl substituents.

molecular wires with increasing number of cumulated carbons and having end-capped ferrocenyl groups (Chart 10) [56]. Depending on the oxidation state of the ferrocene, ferrocenyl cumulenes can exist as cationic $(Fc)_2C=(C)_n=C(Fc)^+$ and neutral $(Fc)_2C=(C)_n=C(Fc)_2$ species. A recent report by Bildstein et al. highlights the present status of the α,ω-diferrocenyl cumulenes [57]. The impetus for designing such systems comes from the fact that the ferrocene units linked directly with the conjugated cumulene chain can serve as stable, fully reversible redox-active centers. Moreover, the Fc-pendants act as inductive donors to the neighboring electron-deficient carbenium center. This not only effects the electronic communication through the cumulene bridge but also affects the reactivity of the sp-carbon chain. Cyclic voltammetry and UV–vis spectroscopy further reveals that the electronic communication between the ferrocenyl termini along the bridging sp-carbon unit depends on the number of cumulated carbons and on the length of the cumulene chain. While the odd-numbered cumulenes $(Fc)_2(C)_n(Fc)_2$ ($n = 3$, 5, etc.) are electronically decoupled, the electronic communication in the even-numbered cumulenes $(Fc)_2(C)_n(Fc)_2$ ($n = 2$, 4, 6, etc.) decreases with increasing chain length.

The ferrocenyl end-groups offer significant steric bulk on the sp-carbon chain of the shorter cumulenes $(Fc)_2(C)_n(Fc)_2$ ($n = 2$–4) thereby preventing electrophilic attack on these carbons. However, it is interesting to note that the ferrocenyl groups of tetraferrocenyl[3]cumulene adopt a *syn*-conformation with regard to the C_4 chain, though an *anti*-arrangement would result in less steric hindrance.

3. The making of linear ferrocenes with unsaturation in the arms

3.1. Routes to ferrocenes with an olefinic backbone

The routes for the preparation of ferrocenes with an olefinic backbone can be classified as follows:

I. Wittig reaction;
II. coupling reactions;
III. organometallic addition reactions;
IV. other miscellaneous reactions.

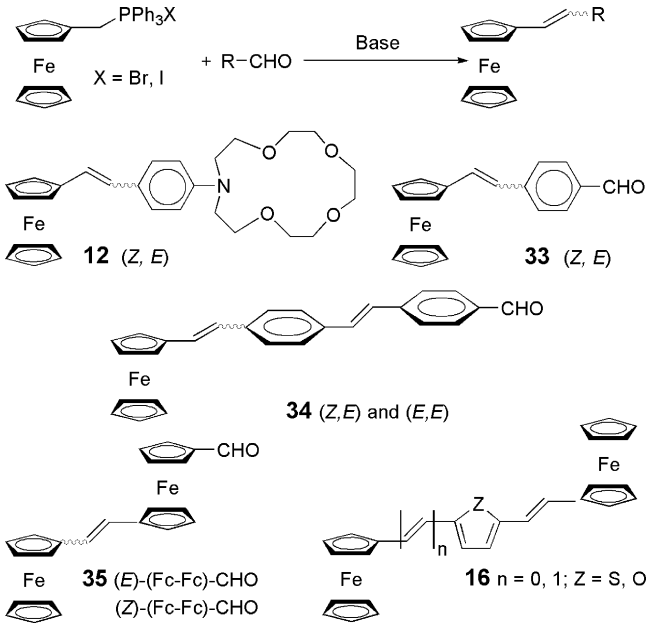

Chart 11. Ferrocenyl alkenes via the Wittig protocol.

3.1.1. Type I: using the Wittig reaction and its variations

The Wittig reaction has been readily used for the synthesis of ferrocenes containing alkene side-arms. Two possible approaches can lead to the desired products. Firstly, a ferrocenyl Wittig salt, e.g. (ferrocenylmethyl)triphenylphosphonium halide in presence of a base can afford the phosphonium ylide which on reaction with different aromatic and heteroaromatic aldehydes gives the corresponding ferrocenyl alkenes mostly as mixtures of isomers; representative examples are shown in Chart 11. With compound **12** a mixture of both the *cis*- and the *trans*-isomers are formed. While PLC on silica gel eluting with 3:2 diethyl ether–petroleum ether gives the *Z*-isomer, direct crystallization of the mixture from a diethyl ether solution affords the *E*-isomer [33]. In the case of **34** a mixture of both the (*Z*,*E*) and (*E*,*E*) isomers are formed, and upon recrystallization from dichloromethane–hexane mixture the isomers are obtained in 10 and 35% yields, respectively [58]. It is to be noted that the compound **33** is formed only when (ferrocenylmethyl)triphenylphosphonium bromide reacts with excess of terephthaldehyde. However, in the presence of equimolar ratio of the reagents a second Wittig reaction of **33** with (ferrocenylmethyl)triphenylphosphonium bromide occurs to give the biferrocene derivative [59].

The biferrocenes with olefinic conjugated bridging ligands such as **35** and those having heteroaromatic spacers **16** are indeed very interesting compounds owing to the interaction between the metal centers and have been readily prepared by reacting (ferrocenylmethyl)triphenylphosphonium bromide with 1,1′-bisformylferrocene and ferrocenyl thienyl or furanyl aldehydes, respectively [31,36].

Alternatively, a phosphorous ylide generated from an organic halide can also couple with ferrocenyl carbonyls to produce the ferrocenyl alkene derivatives (Chart 12). Thus, the short length vinylic chained structures **36**–**38** are synthesized in moderate to excellent yields by treating formylferrocene or

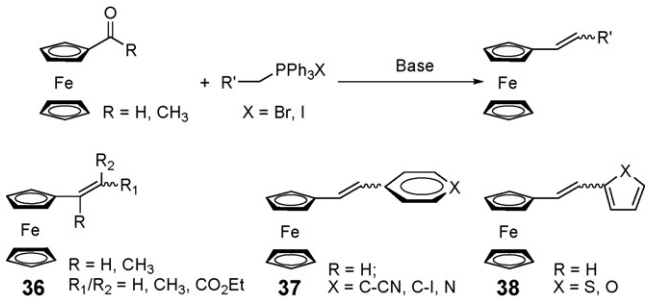

Chart 12. More ferrocenyl alkenes via the Wittig protocol.

acetylferrocene with the corresponding phosphorous ylides [37,58–61].

Using a similar strategy, the 1,1′-disubstituted ferrocenes with olefinic side-arms such as **39** and **40** are obtained as mixture of isomers by the reaction of 1,1′-bisformylferrocene with the corresponding phosphorous ylides (Chart 13) [39,62].

The Wittig methodology has also been extended for the synthesis of biferrocenyl derivatives with phenyl-ethenyl spacers, which are prototype molecular wires. For oligomers **10–11** ($n = 1$) an all *E*-configuration is achieved. However, for the longer chain lengths ($n = 2$, 3) a mixture of stereoisomers are obtained which are difficult to separate.

It is well known that unlike the conventional Wittig reaction, the Horner–Emmons–Wadsworth (HEW) reaction unambiguously affords the *E*-isomers. The latter approach has been utilized to design all-(*E*) ferrocenyl derivatives such as **15**, **34** and **41** in reasonably good yields (Charts 5 and 14) [31,35].

Alternatively, organic phosphonate reagents have also been used in the synthesis of mono and disubstituted vinyl ferrocene derivatives starting from formyl and 1,1′-bisformylferrocene, respectively [63].

As mentioned earlier, the Wittig protocol often produces a mixture of *E*/*Z* stereoisomers; the separation of which is not always easy. This has led to another highly stereoselective variation for the synthesis of vinyl-containing mono and biferrocene derivatives using arsonium salts [64]. Besides stereoselectivity, the method also has the advantages of mild reaction conditions and good yields of the products (62–95%). A promising solvent-free modification has also been developed [65]. Thus, the reaction of formylferrocene and triphenylbenzylphosphonium halide via the solvent-free variation using NaOH base

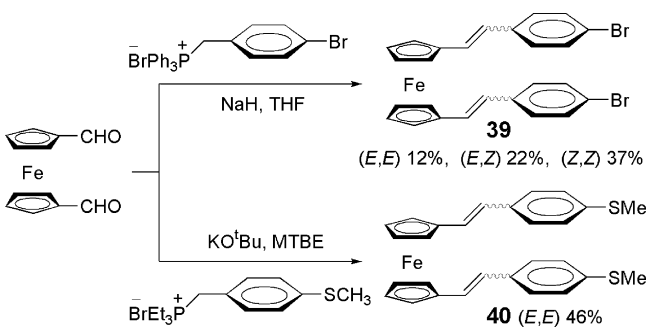

Chart 13. Bisferrocenyl alkenes via the Wittig protocol.

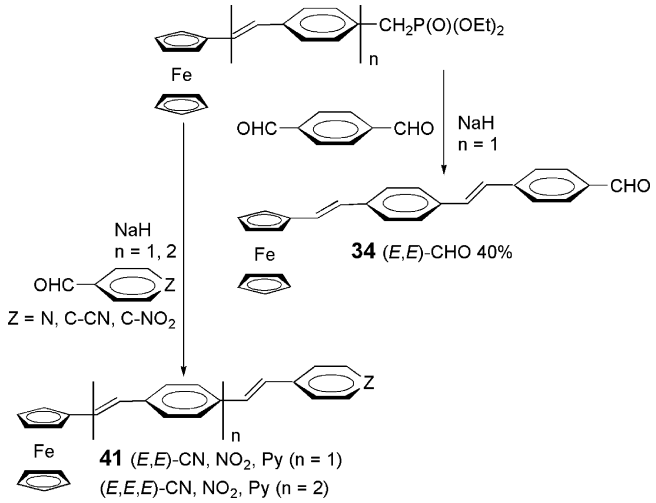

Chart 14. Bisferrocenyl alkenes via the HEW reaction.

produces 1-ferrocenyl-2-phenylethylene in 95% yield in 5 min whereas the same reagents under the conventional Wittig conditions in DMSO solvent and NaH base produces the product in 70% yield in 25 min [60].

3.1.2. Type II: using the coupling reactions

Transition metal assisted carbon–carbon bond forming reactions offer newer avenues to generate ferrocenes with an ene-backbone; most noteworthy of which are the Heck and the McMurry coupling.

3.1.2.1. Heck coupling reaction. The palladium-catalyzed Heck-coupling reaction has been used by us and few other groups for the synthesis of ferrocenyl-based conjugated compounds. While $Pd(OAc)_2$ has been traditionally used as a catalyst for this coupling along with an additive like tetra-alkylammonium salt, and a base in polar aprotic solvents at 80–100 °C, other active and selective Pd-catalysts have also been explored by Peris and co-workers. For example thermally stable *syn*-di(μ-chloro)-bis[*o*-(benzylphenylphosphyno)benzyl]-dipalladium(II) has been used as the catalyst to mediate Heck coupling at an operating temperature of 130 °C to synthesize ferrocenyl-based star-shaped complexes in high yields and in just few hours (Chart 15) [40]. In comparison, traditional Heck

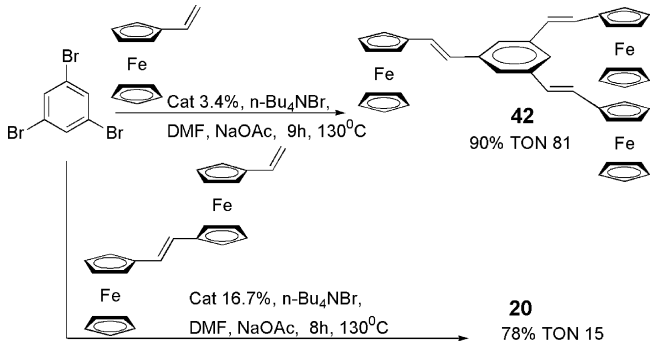

Chart 15. Star-shaped ferrocenylenes via the Heck coupling.

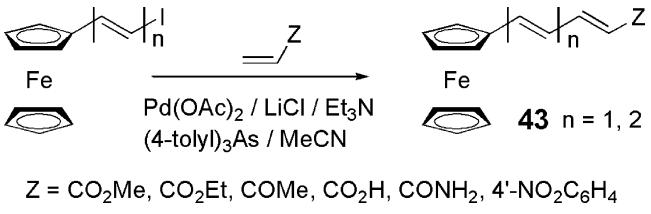

Chart 16. Ferrocene-capped dienes and trienes via the Heck reaction.

catalysts require 2–3 days and afford the product in significantly lower yield. A low turnover number in the case of **20** may be due to an unfavored stereoelectronic effect on consecutive olefination. Synthesis of oligoferrocenyl complexes such as compound **19** (Chart 6) in very high yields are also reported using a thermally stable imidazolyl pincer Pd catalyst [39].

Roy and co-workers demonstrated the Heck-olefination of β-iodovinylferrocene and δ-iodoferrocenyldiene with vinyl substrates for the synthesis of ferrocene-capped dienes in (50–81%) and trienes in (50–87%) isolated yields respectively in the presence of tri(4-tolyl)arsine/palladium acetate/lithium chloride/triethylamine at a much lower temperature of 35–80 °C in MeCN with an excellent all *E*-stereoselectivity (Chart 16) [28].

Thus, it can be concluded that despite the limited availability of the vinyl substrates due to their easy polymerization, the Heck-coupling offers an useful gateway to ferrocenes with olefinic arm and with high stereoselectivity. Further the reactions are also bench-friendly due to cleaner work-ups.

3.1.2.2. McMurry coupling reaction. Only a few reports for the synthesis of ferrocenyl-based olefinic systems by low-valent titanium complex mediated McMurry reaction has been documented till date. The beauty of this reaction however lies in its ability towards doubling of the conjugation length in stereoselective *E*-configuration. For example, compound **45** having ferrocene end groups linked via extended conjugation has been obtained in excellent yields starting from the conjugated ferrocene thienyl or furanyl aldehydes **44** (Chart 17) [36].

The McMurry reaction has also been used as a convenient route for the synthesis of the antitumoral reagent Ferrocifen (Chart 18) [23]. The key step of this synthesis is the reductive coupling of the ferrocenyl ethyl ketone and commercially available 4-methoxybenzophenone with $TiCl_4$/Zn giving the butene **46** in 67% yield. Self-coupling of ferrocenyl ethyl ketone is easily avoided by using large excess of 4-methoxybenzophenone.

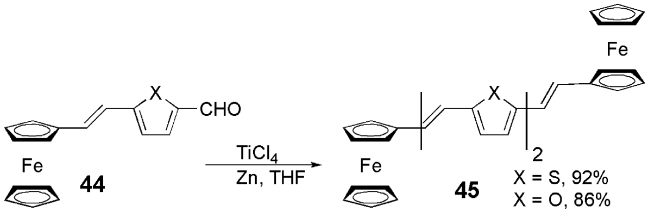

Chart 17. Conjugated ferrocenes via the McMurry coupling.

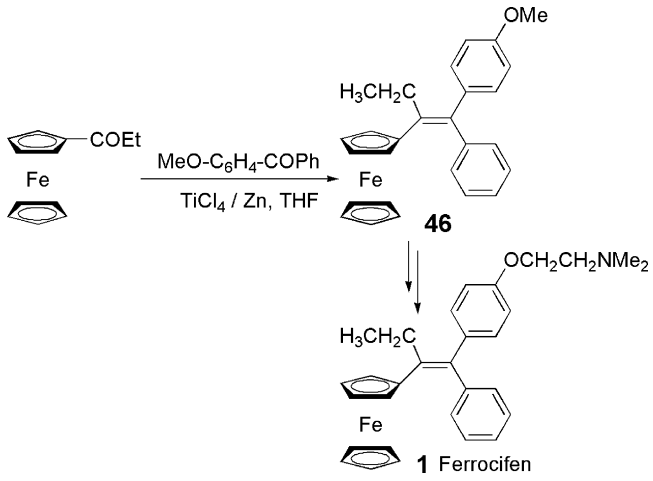

Chart 18. Ferrocifen via the McMurry coupling.

3.1.3. Type III: using the organometallic addition reactions

This method has been mostly exploited for the synthesis of butadienylferrocene. For example, the addition of allyllithium or allylmagnesium bromide to formylferrocene gives 1-ferrocenyl-3-buten-1-ol **47** (Chart 19). With formylferrocene/allyllithium ratio of 1:1 and 1:2 the yields of **47** are 71 and 96%, respectively.

The homoallylic alcohol under suitable conditions ($CuSO_4{\cdot}5H_2O$, acidic Al_2O_3, azeotropic reflux with a strong acid) undergoes facile dehydration to afford 1-ferrocenyl-1,3-butadiene **48** in good yields [66,67].

The butadiene can also be obtained in a single step via refluxing of formylferrocene with allyl bromide in THF in the presence of graphite-supported active zinc (from graphite, $ZnCl_2$ and molten potassium). Here, the goodness of the active zinc determines the yield of the product, which can be as high as 85% with respect to aldehyde [68].

More recently, a simple and expedient SmI_2 promoted 'one-pot' Barbier method is reported for the synthesis of ferrocenyl alkenes **49**, butadienes **4** and enynes **5** from ferrocenyl carbonyls (Chart 20) [26].

The organosamarium halide initially generated by the reaction of a bromide with SmI_2 is amenable to further reaction with ferrocenyl carbonyls to form an alkoxide intermediate; the latter on elimination of $HOSmI_2$ gives the ferrocenyl alkenes. The reaction is tolerant towards a range of ferrocenyl carbonyls including formyl-, acetyl-, benzoyl- and butanoyl-ferrocene.

A more convenient Barbier like one-pot protocol has been recently developed by Roy et al. for the synthesis of ferrocenes with an ene-terminus particularly those pertaining to butadienyl and homoallyl backbone from easily available precursors such as formylferrocene and 1,1′-bisformylferrocene using

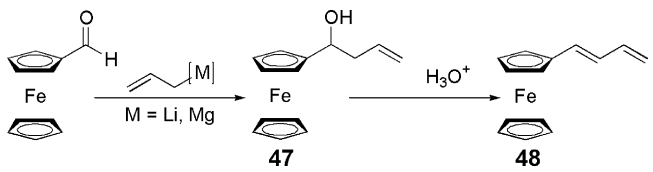

Chart 19. Butadienylferrocene via organometallic addition.

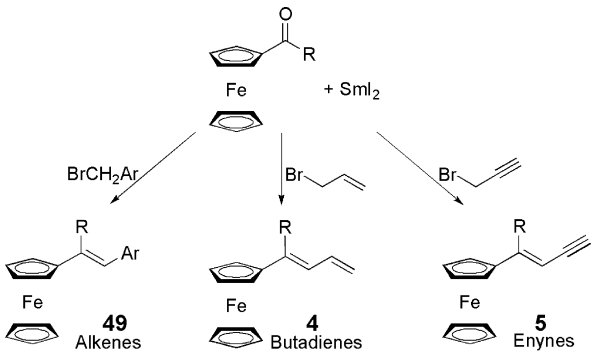

Chart 20. SmI_2 promoted synthesis of ferrocenylenes.

two different bimetallic reagent combination: catalytic d^8, d^{10}-metal complexes and tin(II)halide (SnX_2) or tin(II)oxide (β-SnO) [69–72]. With allyl bromides and using stannous chloride and catalytic cupric chloride in dichloromethane/water, formylferrocene gives 1-ferrocenyl butadiene products **50** in moderate yields (Chart 21). A noteworthy feature of the reaction is the observed 100% γ-regioselectivity affording ferrocenyl derivatives with terminal-unsubstituted olefin linkage.

The reaction can thus be rationalized by a copper(I)-assisted allylstannation mechanism (Chart 22). The steps involved are (a) prior formation of cationic allyltin (**A**); (b) allyl transfer from allyltin to formylferrocene leading to intermediate homoallylic alcohol **HA**; (c) dehydration of homoallylic alcohol leading to the formation of the ferrocenyl butadiene. Indeed pH measurement of the aqueous part of the reaction mixture showed it to be acidic (pH 2–4), which could lead to such in situ dehydration of the homoallyl alcohol. The hypothesis is further supported by the fact that no dehydration takes place in the homoallylic alcohol **51**, which is devoid of any β-hydrogen with respect to the –OH group.

However, the reaction of 1,1′-bisformylferrocene and allyl bromides under similar conditions gave the oxa-[3]ferrocenophane products (Chart 23) via a cooperative dehydration mechanism of the respective diols under acid catalysis (Chart 24) [71]. This is probably due to the extraordinary stability of the ferrocenylcarbinyl cation intermediate (**B**) which undergoes intramolecular trapping by the second hydroxyl group resulting into the thermodynamically stable ferrocenophanes [73]. Like in the reaction of formylferrocene, in **53** also linear dehydration was arrested along with complete restriction of internal cooperative dehydration.

A similar β-SnO promoted allylation of formylferrocene with allyl bromides in refluxing THF–H_2O (9:1, v/v) catalyzed by Pd(0)/Pt(II) formed the ferrocenyl butadienes in moderate yield (Chart 25) [72].

The products are formed via a redox-transmetallation strategy promoting allyl transfer from allyl-palladium and platinum (**C**) to tetragonal tin(II) oxide (β-SnO), and further utilizing the in situ generated allylstannane (**D**) towards allylation of ferrocenyl aldehydes (Chart 26).

However with 1,1′-bisformylferrocene only the monoallylated products could be isolated in albeit poor yields (Chart 27). Only with 1-bromo-3-methyl-but-2-ene the mono alcohol product 1-(2,2-dimethyl-but-3-en-1-ol)-1′-formylferrocene **55** was obtained in 60% isolated yield. The butadienes result from in situ dehydration of the corresponding homoallylic alcohols formed by the γ-regioselective allylation pathway.

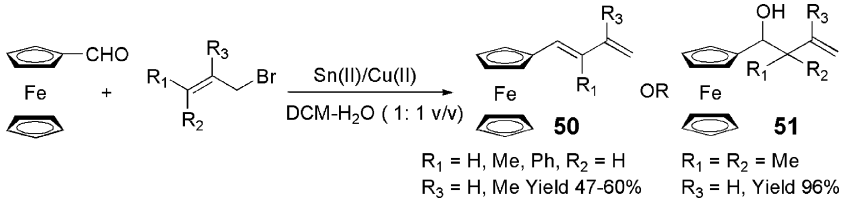

Chart 21. Allylation of formylferrocene using Sn(II)/Cu(II) in DCM–H_2O.

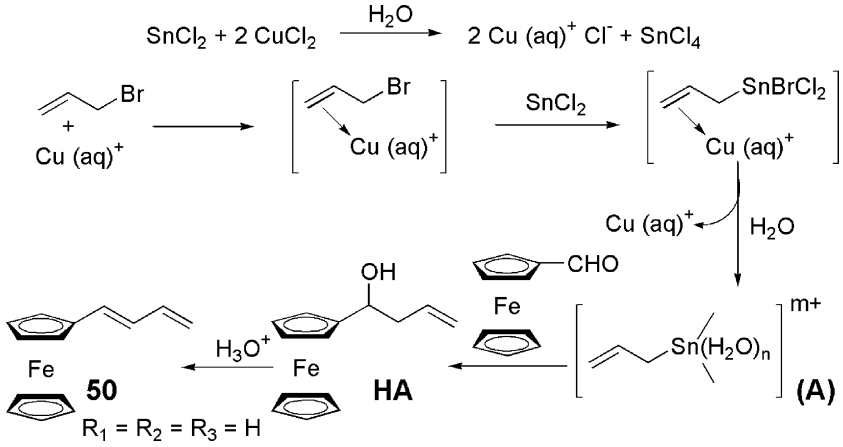

Chart 22. Copper(I)-assisted allylstannation mechanism.

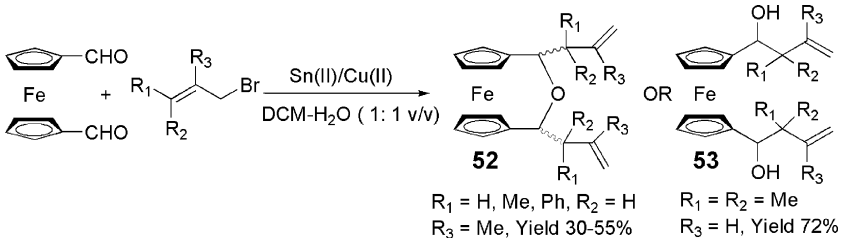

Chart 23. Allylation of 1,1′-bisformylferrocene using Sn(II)/Cu(II) in DCM–H_2O.

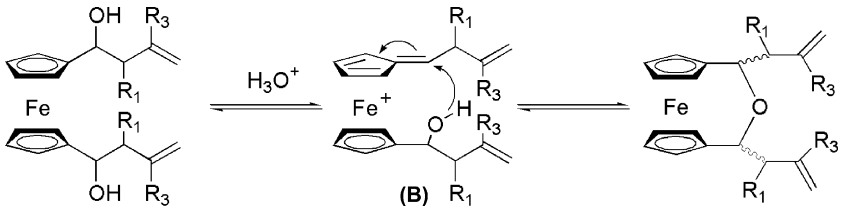

Chart 24. Cooperative dehydration mechanism.

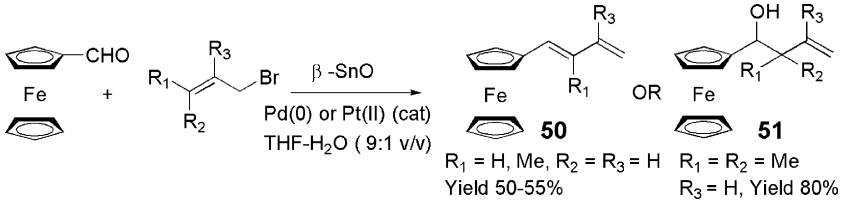

Chart 25. Allylation of formylferrocene using β-SnO and Pd(0)/Pt(II) in THF–H_2O.

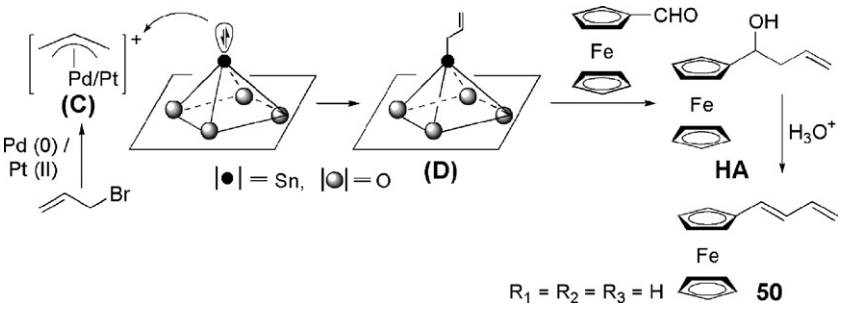

Chart 26. Formation of ferrocenyl butadienes via σ-allyltin(IV) intermediate.

Further condensation of the monoallylated ferrocenyl aldehyde **55** with *p*-phenylenediamine gave a binuclear ferrocenyl alcohol **56**, which can be viewed as a potential precursor for the construction of a multinuclear ferrocenophane with extended nitrogen containing π-conjugated aromatic bridge between the two ferrocene units (Chart 28). Such compounds may also serve as suitable candidates for the study of electron-transfer between the metal centers via through bond processes [72].

3.1.4. Type IV: using other miscellaneous reactions

Routes to the ferrocenylenes, which are conceptually distinct from those described so far have been accrued here and are presented below.

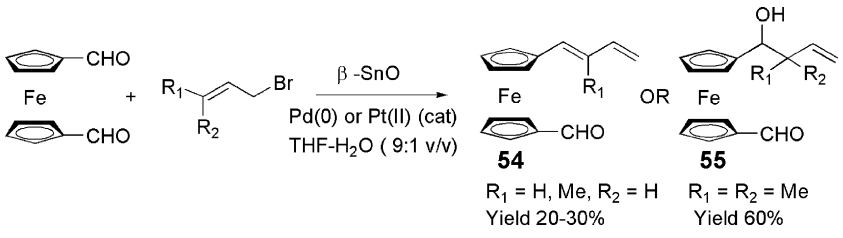

Chart 27. Allylation of 1,1′-bisformylferrocene using β-SnO and Pd(0)/Pt(II) in THF–H_2O.

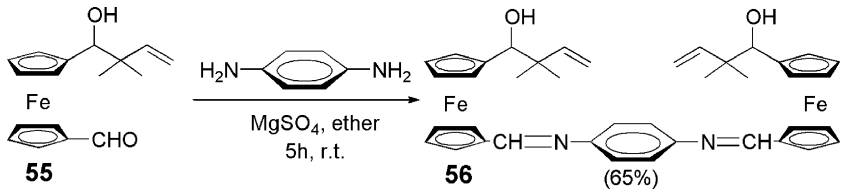

Chart 28. Synthesis of a binuclear ferrocenyl homoallylic alcohol.

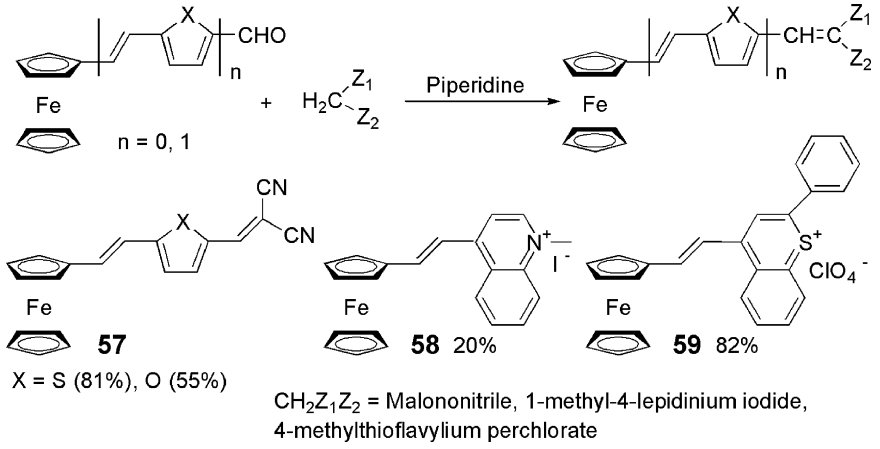

Chart 29. Ferrocenylenes via the Knoevenagel condensation.

Many push–pull ferrocenylenes having electron-withdrawing end-cap have been synthesized from ferrocenyl aldehydes under the Knoevenagel condition. Some key structures are shown in Chart 29 [59,74]. These conjugated ferrocene compounds with heterocyclic acceptors show significant second-order NLO properties.

While the reaction of the appropriate ferrocene aldehydes with malononitrile and *N*-methyllepidinium iodide in presence of catalytic amount of piperidine base led to the formation of **57** and **58**, respectively, decomposition of **59** is observed on reacting ferrocenecarboxaldehyde with 4-methylthioflavylium perchlorate under the same condition. However, **59** can be obtained in analytically pure form by direct precipitation from the reaction mixture when no base is used. Recently, the Knoevenagel condensation of formylferrocene with a series of active methylene compounds have been tested in a solvent-free environment over a large number of inorganic supports—Brockman II grade alumina and silica gel were found to be superior leading to products in high yields (>70–98%) [75].

The ring opening metathesis polymerization (ROMP) has been used solely for the synthesis of conjugated polymers containing ferrocenylene units. Ferrocenophanes and strained *ansa*-ferrocenes are the common precursors for this reaction. Buretea and Tilley reported the synthesis of polyferrocenylenevinylene (PFV), **61** an organometallic analogue of polyphenylenevinylene (PPV), via ROMP of strained vinylene-bridged *ansa*-ferrocene **60** using Schrock's carbene complex (Chart 30) [76].

Lee and co-workers obtained the soluble, high molecular weight π-conjugated ferrocenylene polymer **63** (M_w as high as 300,000) from a new ferrocenophane, 1,1′-(1-*tert*-butyl-1,3-butadienylene)ferrocene **62** using a tungsten-based metathesis

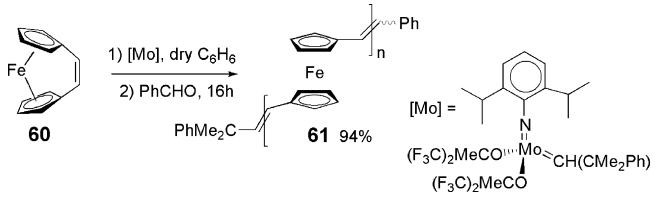

Chart 30. Polyferrocenylenevinylene via ROMP using Schrock's carbene.

catalyst (Chart 31) [77]. It is seen that the molecular weight of **63** increases qualitatively with the increase in monomer-to-catalyst ratio. In contrast, the molecular weight of the polymer obtained from corresponding aryl-substituted analogues are lower and cannot be varied by varying the monomer-to-catalyst ratio due to less bond angle strain in the reacting ferrocenophane.

In a recent report, ferrocenyl acetylene has been successfully polymerized to produce the electro-active polyene, polyferrocenylacetylene (PFA) containing ferrocene units in the backbone using the classical metathesis catalyst $W(CO)_6/CCl_4/h\nu$ [29].

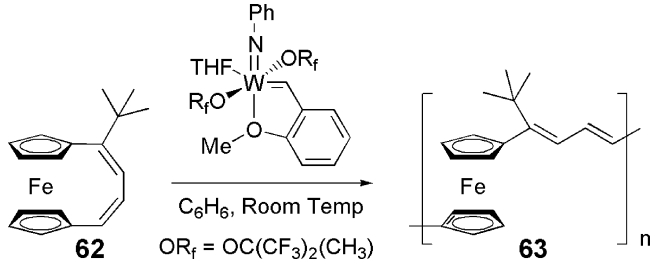

Chart 31. Ferrocenylene polymer via ROMP using tungsten catalyst.

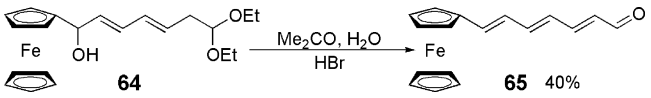

Chart 32. Ferrocenyl triene via the elimination reaction.

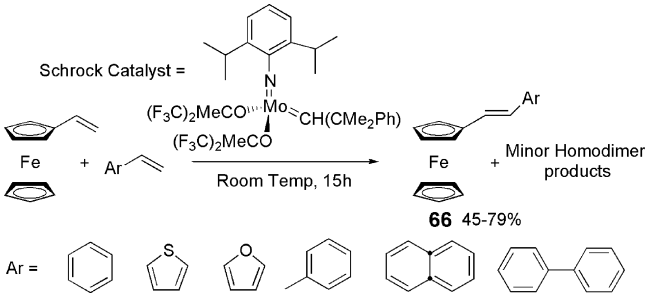

Chart 33. Ferrocenyl alkenes via the cross-metathesis reaction.

Dehydration of ferrocenyl alcohols in presence of suitable agents is a convenient way of producing ferrocenyl alkenes. Many dehydrating reagents such as neutral Al_2O_3, acidic Al_2O_3, $Fe_2(CO)_9$, methanesulfonyl chloride and triethylamine have been attempted by different groups to obtain the ferrocenyl alkenes in stereoselective configuration [78]. In a similar approach compound **65** bearing a conjugated triene chain attached to a Cp ring is obtained by the hydrolysis and subsequent elimination of the alkanoyl compound **64** by refluxing in a mixture of acetone, water and hydrogen bromide (Chart 32) [27].

Metathesis reaction has also been applied for the synthesis of ferrocenyl alkenes. Thus, π-conjugated 1-aryl-2-ferrocenylethylene heterodimer products **66** were obtained via cross-metathesis of vinylferrocene and a series of vinylarenes using a homogeneous metathesis Schrock catalyst (Chart 33) [79].

Homocoupling of haloarenes to form biarenes using stoichiometric Ni(0) complexes is an easy way for extending molecular conjugation. A similar strategy has been utilized for the coupling of (*E*)-1-ferrocenyl-2-(*p*-iodophenyl)ethene **67** using tristriphenylnickel(0) prepared in situ by the reduction of dichlorobis(triphenyl-phosphine)nickel(II) with zinc in tetrahydrofuran leading to the synthesis of the π-conjugated biferrocene **17** (Chart 34) [37].

A modified Clemmensen reduction of diferrocenyl ketone using zinc and trimethylchlorosilane has been successfully used for the synthesis of tetra-ferrocenylethylene **18** in 70% yield [38]. Unlike the traditional Clemmensen reduction, here the proton has been replaced by a silicon electrophile whose high oxophilicity removes the carbonyl oxygen as hexamethyldisiloxane generating an organozinc carbenoid, leading to the product in a manner similar to that of the McMurry reaction (Chart 35). This method is highly preferred owing to the availability of starting materials, convenience of reaction conditions and higher yield of the product. Note that the byproduct tetraferrocenylethane is formed in only 10% yield.

Recently, we have attempted a facile transesterification route using the mild base tetrabutylammonium hydroxide as catalyst in neat alcohol under ambient condition, for the synthesis of new ferrocenylene esters **68** in general, and 1,1′-bis ferrocenylene esters **69** in particular [80]. The reaction was applied successfully to ferrocenyl ethylesters having unsaturated backbone either at one or both the Cp rings (Charts 36 and 37).

Further, the route has been extended for the synthesis of a hydroxyl capped ferrocenylene ester **70** using 1-hydroxy,3-(isothiocyanato)tetrabenzyldistannoxane (**E**) as catalyst (Chart 38).

The ring closing metathesis (RCM) of an ester also allowed to close the open-arms affording a ferrocenophane **71** with an ene-backbone (Chart 39).

3.2. Routes to ferrocenes with an acetylenic backbone

Several syntheses of ferrocenes with an acetylenic backbone using the cross-coupling reactions such as Sonogashira coupling, Negishi coupling, Glaser coupling, Stille coupling and

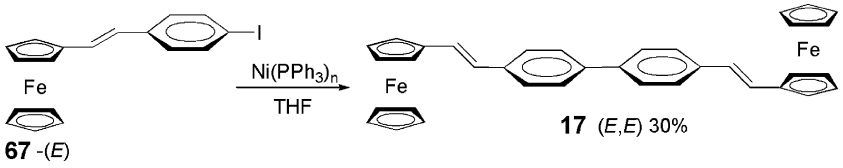

Chart 34. Route to ferrocenes with an extended conjugation.

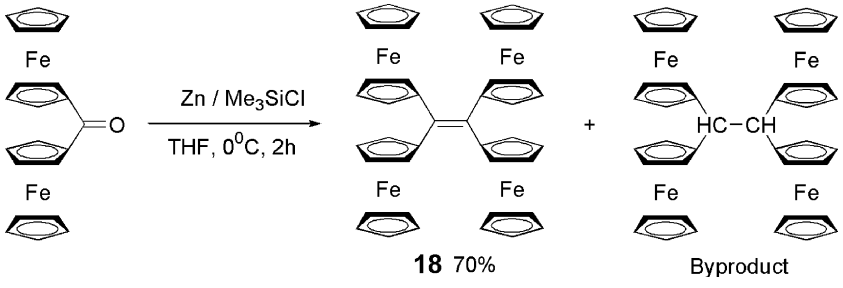

Chart 35. Perferrocenylated alkene via the Clemmensen reduction.

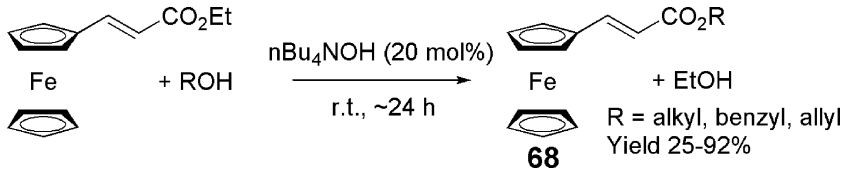

Chart 36. Synthesis of ferrocenylene monoesters.

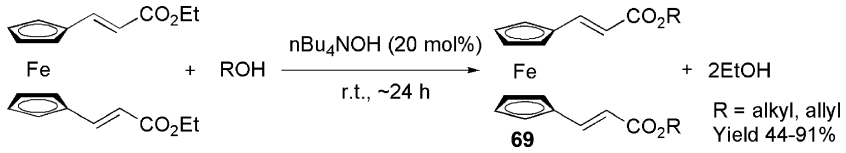

Chart 37. Synthesis of 1,1′-bisferrocenylene esters.

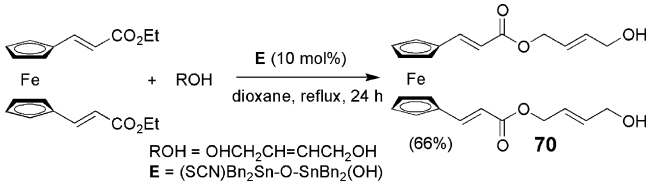

Chart 38. Synthesis of a hydroxyl capped ferrocenylene ester.

Stephens–Castro coupling have been reported in the literature. In this section, we closely look into these routes.

The Sonogashira coupling of ethynylferrocene derivatives with aromatic/hetero-aromatic halides using catalytic amounts of Pd(II) and CuI and an amine base has led to many ferrocenyl derivatives with unsaturated acetylenic side-arms. Some selected molecules prepared by this method are shown in Chart 40.

Often the reaction is accompanied by a minor product arising from the homocoupling of the acetylene units, which can be avoided by maintaining a perfectly anaerobic condition. Structure **72** shows that the reaction tolerates both electron-withdrawing as well as electron-donating substituents on the aromatic ring [44]. The reaction of ferrocenylacetylene with 4-$BrC_6H_4C{\equiv}N$ in 1:1 molar ratio in the presence of catalytic amounts of $PdCl_2(PPh_3)_2$/CuI in diisopropylamine as solvent leads to the compound **72** (R = H, R_1 = CN) in 84% yield [45]. This compound with an additional C≡N ligating site serves as the basis for the preparation of oligonuclear ferrocene-based transition metal complexes. Structure **24** (Chart 7) shows such a trimetallic complex. A similar co-ordination site is also provided by the dangling pyridine unit in compound **73** prepared by the coupling of 1-(ferrocenylethynyl)-4-ethynylbenzene with 4-bromopyridine catalyzed by 3 mol% of $PdCl_2(PPh_3)_2$ and CuI in diethylamine [47]. Structures **74–76** are all prepared

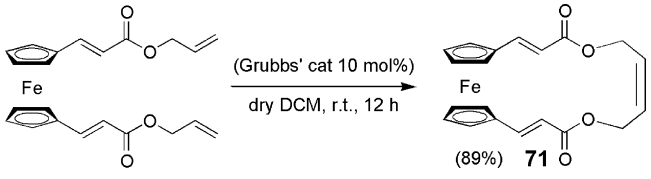

Chart 39. Synthesis route to a ferrocenophane.

by coupling ethynylferrocene with the appropriate monobromooligothiophene unit using $PdCl_2(PPh_3)_2$ and CuI catalysts and diisopropyl-amine in tetrahydrofuran solvent [51].

The Sonogashira coupling has also been extended to the biferrocene compounds **29**, by reacting ethynylferrocene with the corresponding dibromoaryl precursors in the presence of Pd(II)–CuI catalysts in refluxing diisopropylamine (Chart 41) [50–52]. At times, substituting Cu(I) catalyst by Cu(II) results in lower yields of the product. For example, the yield of 2,5-bis(ferrocenylethynyl)thiophene using Cu(I) and Cu(II) catalysts are 71 and 50%, respectively.

Successive Sonogashira coupling of iodoferrocene with acetylenic substrates have been achieved for the reaction of iodoferrocene with 1,4-diethynylbenzene in the presence of catalytic amounts of $PdCl_2((PPh_3)_2)$/$Cu(OAc)_2$ in HN^iPr_2 at 90 °C to give the complex **77** in 95% yield (Chart 42) [81].

Iodoferrocene has also been the starting material for the synthesis of many ferrocenylacetylene derivatives through various coupling pathways (Chart 43) [82–84]. Thus, compound **78** has been synthesized by the Pd(0)-catalyzed Stille coupling using 4-pyridyl(trimethylstannyl)acetylene and iodoferrocene, while **79** is prepared by a Pd(0)-catalyzed Negishi coupling of the organozinc component with iodoferrocene [47]. The Castro and Stephens coupling approach is used to synthesize arylferrocenylethynes **80** in 26–50% yields by reacting the corresponding copper arylacetylide with iodoferrocene in refluxing DMF rather than usual pyridine as solvent. It is noteworthy that refluxing equimolar amounts of iodoferrocene and cuprous phenylacetylide in pyridine for 8 h under nitrogen provides the ferrocenylphenylacetylene (**80**, Ar=Ph) in 84% yield. In an analogous manner, coupling of iodoferrocene and cuprous ferrocenylacetylide produces the diferrocenylacetylene (**80**, $Ar{=}FeC_{10}H_9$) in 85% yield.

Extension of conjugation between the two ferrocene centers via an acetylene unit has also been achieved using the oxidative Glaser coupling of (*E*) and (*Z*)-**81** respectively, leading to diynes (*E*,*E*) and (*Z*,*Z*)-**82** in excellent yields (Chart 44) [37].

3.3. Routes to ferrocenes with a cumulenic backbone

Though very few ferrocenyl substituted allenes containing only one or two ferrocenyl groups are reported in the literature

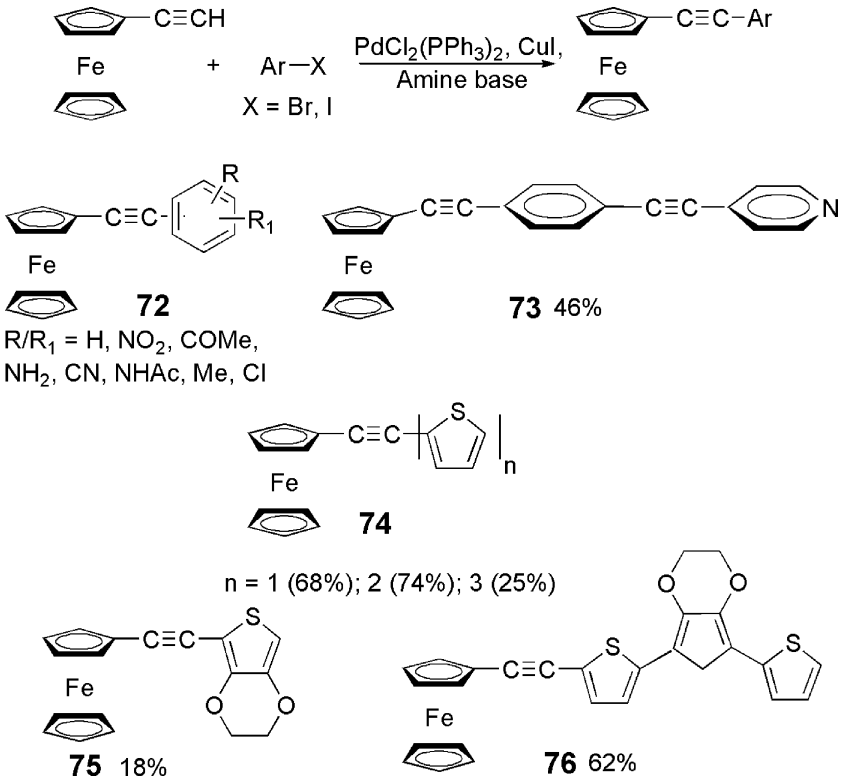

Chart 40. Monoferrocenyl alkynes via the Sonogashira coupling.

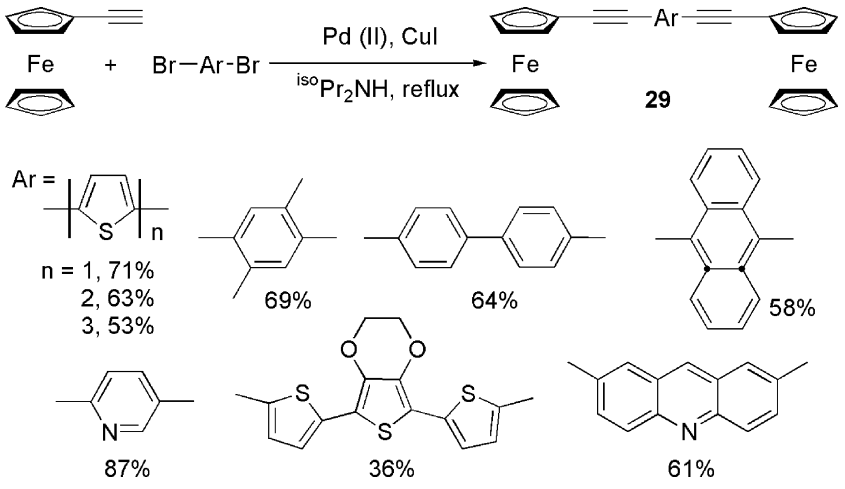

Chart 41. Bisferrocenyl alkynes from ethynylferrocene via the Sonogashira coupling.

till date, significant progress has been made in the synthesis of perferrocenylated cumulenes with diferrocenyl ketone as the key starting material. Since the subject has been recently reviewed [56], the synthetic routes for a few tetraferrocenylated cumulenes are briefly discussed here (Chart 45). Alkynylation of the diferrocenyl ketone **83** with ferrocenyl acetylene produces the propynol **84**, which undergoes water elimination on protonation to form the cumulenic carbenium salts. These allenylium/propargylium salts are used as the progenitor of tetraferrocenylallene. However, alkynylation of **83** with

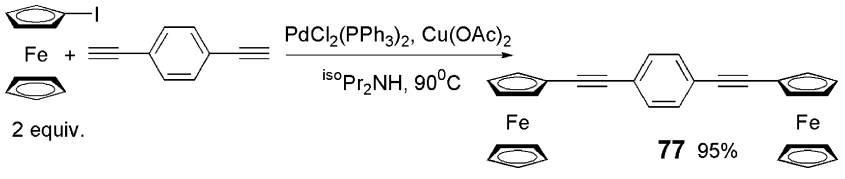

Chart 42. Bisferrocenyl complex from iodoferrocene via the Sonogashira coupling.

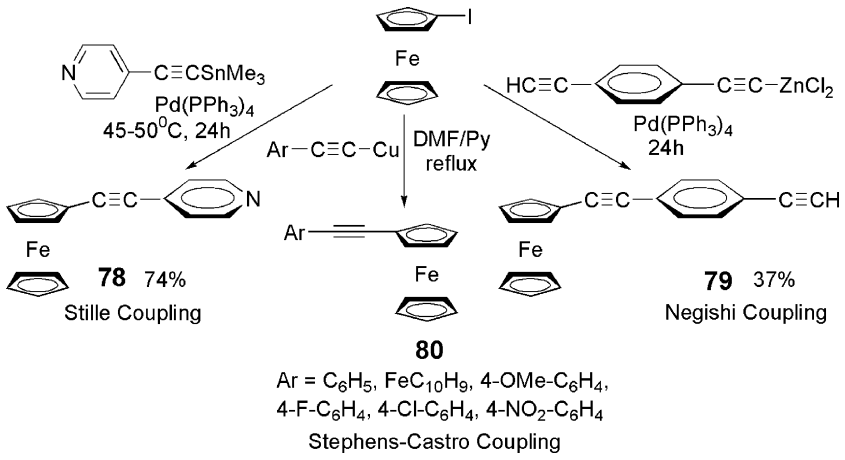

Chart 43. Ferrocenylacetylenes from iodoferrocene.

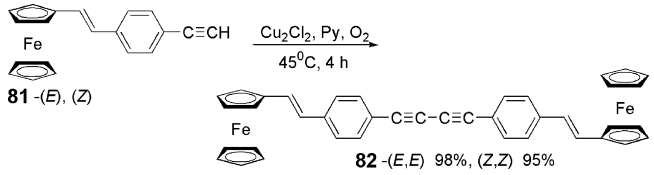

Chart 44. Oxidative dimerization of ferrocenylacetylene units.

trimethylsilylacetylene and subsequent methylation gives the diferrocenylmethoxypropyne **85**. Nucleophilic addition of metallated **85** to diferrocenyl ketone and subsequent reduction with stannous chloride finally affords the [3]cumulene. Interestingly, other reducing agents (Zn/trimethylchlorosilane, SmI_2, $Fe(CO)_5$, $Fe_2(CO)_9$ low-valent titanium) give either only traces of the product or over-reduced products like tetraferrocenylbutadiene. Similar reactions of the metallated methyl protected hydroxybutyne **86** with **83** leads to 1,1,5,5-tetraferrocenyl-1-hydroxy-5-methoxy-pent-2-yne. Most interestingly, elimination of water and methanol with only one equivalent of proton produces the conjugate acid of the desired tetraferrocenyl[4]cumulene, which on deprotonation with potassium *tert*-butoxide forms tetraferrocenyl[4]cumulene in 46% yield. Similar synthetic strategies along with cross-coupling of the alkyne compounds with acetylides or dimerization of the zwitterions formed by deprotonation of the propynols lead to the synthesis of the higher cumulenes.

4. Tuning the properties of ferrocenes with an unsaturated backbone

Ferrocene derivatives with linear, unsaturated side-arms show altered/unique properties compared to their saturated analogues. Some of these properties include electrical conductivity, thermal stability, magnetic, electronic, redox, and non-linear optical behavior. This can be accounted to the electronic interaction of both metal- and ligand-based orbitals of ferrocene platform with the orbitals of the π-conjugated substituents in the side-chain. Not surprisingly, some of the properties are dramatically

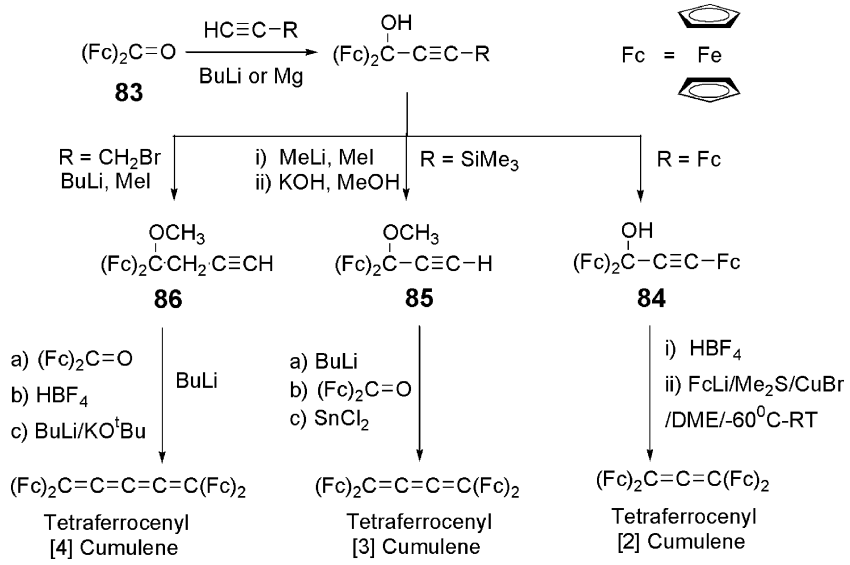

Chart 45. Route to cumulenes with ferrocenyl termini.

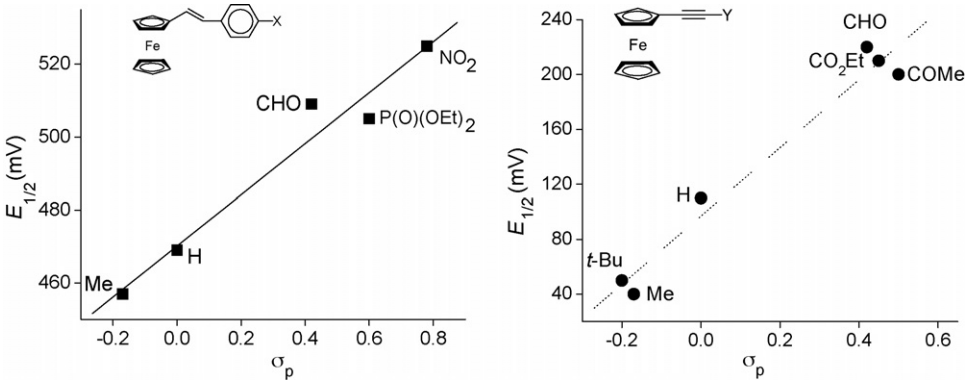

Chart 46. Substituents effect on redox behavior of ferrocene bearing an unsaturated side-arm.

dependent on the chemical nature and length of the conjugated substituents. In this section, we closely look into these properties individually with special emphasis to the electronic, redox and optical effects of ferrocenes with an olefinic and an acetylenic conjugation. As interesting reviews on the properties of ferrocenyl cumulenes are available recently [56,57], their properties are not touched upon.

4.1. Redox behavior of ferrocenes with an unsaturated backbone

Electrochemistry has been extensively used to study the property sequence that occurs on changing the length and nature of the conjugated substituents attached to the ferrocene platform. Chain lengthening of the π-conjugated system results in a non-linear decrease of the redox potentials due to charge delocalization and stabilization of the ferrocenium form. For example the $E_{1/2}$ values of Fc(CH=CH)$_n$–CO$_2$Me are 0.72, 0.59, 0.49 and 0.46 V for $n = 0, 1, 2, 3$, respectively [28]. The non-linear effect is also observed in ferrocenes with repeating phenyl-ethenyl unit, such as in Fc(CH=CH–C$_6$H$_4$)$_n$–CN [31]. Also noteworthy is the ease of oxidation at lower potential in effectively conjugated *E*-isomer than the corresponding *Z*-isomer, as represented by Fc(CH=CH–C$_6$H$_4$)$_2$–CN–W(CO)$_5$ ($E_{1/2}$ = 435 V for *E*,*E*-; 450 V for *E*,*Z*-) [58]. Good dependence of chain lengthening and redox potential is also observed in the ferrocene dimers with olefinic and acetylenic bridges. Due to the two redox centers, these complexes are expected to show two redox potentials—the peak separation ($\Delta E_{1/2}$) indicates the extent of internuclear electron transfer. Dependence of electron transfer with chain length is clearly established in the dimer Fc(CH=CH)$_n$Fc (n = 1–6). With increasing n, $\Delta E_{1/2}$ decreases, and for $n = 4$ it becomes zero. Similar decrease in $\Delta E_{1/2}$ values is also prominent in the biferrocenes with acetylenic bridges such as Fc(CH≡CH)$_n$Fc (n = 1, 2) [85,86].

The next notable feature is the dependence of Fc/Fc$^+$ redox potential on the chemical nature of the conjugated side-arm in the ferrocene derivatives. Electron-withdrawing fragments attached to the terminus of the conjugated arm stabilize the neutral Fc-form over the cationic Fc$^+$-form, and results in an anodic shift of the redox-wave compared to that of the free ferrocene. This view is further supported by the linear relationship in the plot of $E_{1/2}$ versus Hammett σ_p values of substituents in the ferrocenyl derivatives having a phenyl-ethenyl and an acetylenic spacer, respectively (Chart 46) [87,88].

4.2. Electronic properties of ferrocenes with an unsaturated backbone

The electronic structure of ferrocene includes three highest filled levels resulting from d_{xy}, $d_{x^2-y^2}$ (e_{2g}) and d_z^2 (a_{1g}) orbitals, which are essentially metal-based, while the next highest orbitals (e_{1u}) are principally ligand-based. The molecular orbitals resulting from the d_{xz} and d_{yz} bonding interactions (e_{1g}) are occupied, while the antibonding counterpart (e^*_{1g}) remains vacant. The complete energy level diagram of all the resulting molecular orbitals and those with maximum d-character (highlighted in the box) are shown in Chart 47 [89].

Generally, two prominent bands are observed for ferrocenyl compounds in the visible region. In agreement with previous experimental works and theoretical treatment, the higher energy band (300–390 nm) is assigned to a π–π* intra-ligand transition, and the less energetic band (400–500 nm) is assigned to a metal to ligand charge-transfer band (MLCT). In addition to these, another very weak band at higher wavelength (about 500 nm), assigned as d–d transition, is sometimes discernible as a shoulder on the MLCT band [31].

Attaching a conjugated system to ferrocene causes significant perturbation of the ligand-based (e_{1u}) orbitals. With increasing conjugation length, the energy of the π* orbital is lowered resulting in red shift of the π–π* transition. Thus, for the compound Fc(CH=CH)$_n$–CO$_2$H, λ_{max} varies as 295 nm (n = 1), 319 nm (n = 2) and 346 nm (n = 3) [28]. Also notable is the bathochromic shift of λ_{max} upon polymerization of **62** (λ_{max} = 240 nm) to **63** (λ_{max} = 320 nm), suggesting greater degree of conjugation in the polymer [90]. An increase in wavelength with degree of conjugation is also observed for the ferrocenyl derivatives having a phenyl-ethenyl and a phenyl-ethynyl spacers. For example in Fc(CH=CH–C$_6$H$_4$)$_n$–NO$_2$, λ_{max} varies as 363 nm (n = 1) and 388 nm (n = 2) [31].

Red shift of both the higher and the lower energy bands also results on attaching an electron-withdrawing moiety to

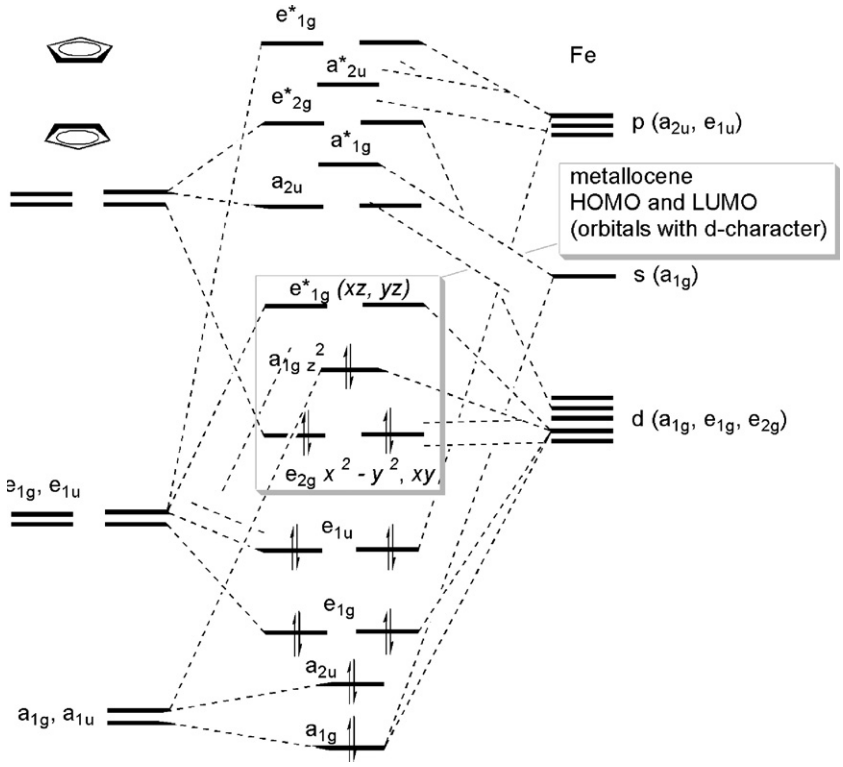

Chart 47. Molecular orbital energy levels in ferrocene.

the conjugated side-arm. These changes are more prominent in the case of *E*-isomers due to the greater degree of charge-transfer along the conjugated chain. For example, in compound Fc(CH=CH–C_6H_4)$_n$–CN ($n=2$) the λ_{max} values corresponding to (*E*,*E*)-isomer, and (*E*,*Z*)-isomer are 369, and 340 nm, respectively. Note that compound (*E*,*E*)-Fc(CH=CH–C_6H_4)$_n$–NO_2 ($n=2$) with a stronger electron-withdrawing –NO_2 group exhibits λ_{max} at a much higher wavelength of 388 nm than the corresponding nitrile derivative [31]. A negative solvatochromism indicated by hypsochromic shifts of both the high and low energy absorption bands to lower wavelengths is also observed for most ferrocenyl-based phenyl-ethenyl conjugated compounds on going from a less polar to a more polar solvent [58]. Since solvatochromic behavior reflects the polarizability of a chromophore, studying the electronic spectra forms an important means to measure the magnitude of non-linear properties in a donor–acceptor bridged molecule.

4.3. Non-linear optical properties of ferrocenes with an unsaturated backbone

The report by Green et al. revealing good second-harmonic generation (SHG) for *cis*-[1-ferrocenyl-2-(4-nitrophenyl)ethylene] [91], prompted many research groups to develop ferrocene-based push–pull molecules and to study their suitability for non-linear optical effects. As a result of these efforts a wide variety of ferrocene donor–conjugated bridge–acceptor 'push–pull' non-linear optical (NLO) compounds showing good second harmonic generation are known, and the subject is well-reviewed [30,92,93]. Therefore, only the important non-linear optical properties arising out of structural variations in the π-conjugated ferrocene derivatives are highlighted below.

Increasing the length of the π-bridge in the polyene chain results in an enhanced second-order NLO response (β). Thus, in Fc(CH=CH)$_n$–CO_2Me the SHG efficiency ($\beta \times 10^{-30}$ in $cm^5\ esu^{-1}$) for $n=1$, 2, and 3 are 35, 39 and 42, respectively [28]. Similarly, for all-*E*-isomers of Fc(CH=CH)$_n$–Ar (Ar = 4-nitrophenyl), the β-values are 31×10^{-30} esu for $n=1$, and 403×10^{-30} esu for $n=2$, respectively. Interestingly the corresponding *Z*-isomer show much reduced SHG response ($\beta = 122 \times 10^{-30}$ esu for $n=2$) due to diminished electronic coupling between the donor (ferrocenyl) and the acceptor [31]. Also noteworthy is the fact that greater the electronic asymmetry between donor and acceptor groups, higher is the SHG response. For example, compared to the 4-nitrophenyl analogue of (*E*,*E*)-Fc(CH=CH)$_2$–Ar, the 4-carbomethoxyphenyl derivative shows lower SHG efficiency ($\beta = 39 \times 10^{-30}$ esu). The donor–acceptor interaction can also be accentuated by metal containing acceptors resulting in enhanced NLO effect. This is well illustrated by 1-ferrocenyl-2-(4-pyridyl)-ethylene ($\beta = 21 \times 10^{-30}$ esu) and its N-coordinated derivatives with $M(CO)_5$ ($\beta = 63$, 95 and 101×10^{-30} esu for M = Cr, Mo, W, respectively) [31]. Similar β-enhancement is observed for the triple bond conjugated metal coordinated compound **28** [49]. Not surprisingly, the pentamethylcyclo-pentadienyl derivatives (Cp^*–Fe) show greater NLO response compared to their Cp-analogues due to an increase in donor strength of the ferrocene platform in the former [94].

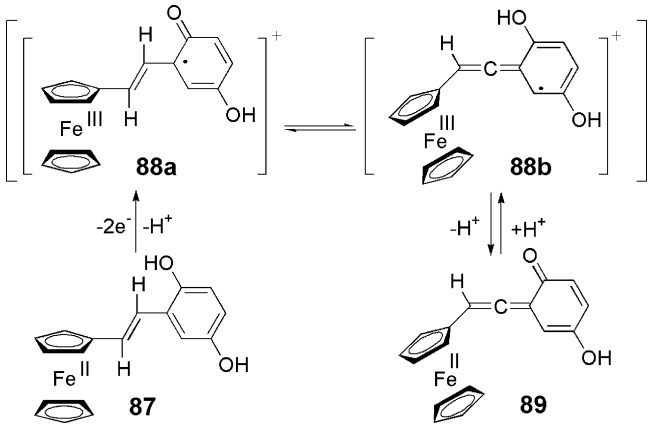

Chart 48. Structural change induced magnetic property in ferrocene.

4.4. Other properties of ferrocenes with an unsaturated backbone

Besides those discussed above, ferrocenes with an unsaturated backbone also possess some other unique properties. For instance, substituents on poly(ferrocenylene) backbone influences both the thermal stability and the thermal transition behavior of the ferrocene-based π-conjugated polymers. Similar tuning of electrical conductivity along the π-conjugated polyferrocenylene chain is also possible by selective substitution on the polymer backbone [77]. For example, the iodine-doped polymers of the unsaturated aryl-substituted ferrocenophanes 1,1′-(1-phenylbuta-1,3-diene-1,4-diyl)ferrocene and 1,1′-(1-mesityl-buta-1,3-diene-1,4-diyl)ferrocene are of the order $10^{-5}\,S\,cm^{-1}$, which is much lower than those reported for either poly(ferrocenylenevinylene) ($10^{-3}\,S\,cm^{-1}$) or poly(ferrocenylenedivinylene) ($10^{-4}\,S\,cm^{-1}$). A possible interpretation for this reduced conductivity is that the aryl substituents induce interchain hopping as a dominant mechanism for conductivity rather than interchain conduction through the polymer backbone.

Tunable magnetic property is observed by the unusual structural change of a quinonoid compound linked to ferrocene by a vinylene spacer **87** to a novel allene and quinonoid structure **89** by two-electron oxidation and two-proton elimination in protic media (Chart 48) [95]. The ESR spectrum of **89** exhibits a well-resolved signal ($g = 3.97$, $g_{\perp} = 1.64$) at 6.4 K by conversion to the paramagnetic semiquinone-ferrocenium compound **88a** through protonation.

5. Concluding remarks

The over half century old ferrocene chemistry has witnessed the emergence of many structural motifs built around the ferrocene platform. The present review highlighted on the motifs bearing unsaturated side-arms on one or both the cyclopentadienyl rings. The discussion reveals that such motifs can be generated by suitably grafting ene, phenyl(ethylene), acetylenic or cumulenic spacers between two ferrocenes or between a ferrocene and an organic group. Examples of motifs having conjugated all-π arms are very few and are viewed as promising candidates in building nano-architectures. On the other hand, compounds having an ene-terminus in the arm(s) are building blocks for metathesis and polymerization reactions leading to organometallic oligo/polymers or metallophanes. It is now generally accepted that an unsaturated appendage acts as a messenger to facilitate communication between the arm and the redox center. This leads to synergistic perturbation of electronic, opto-electronic and electrochemical properties of the molecule. Not surprisingly, compounds belonging to such motif find end-applications in diverse areas ranging from metallomesogens, NLO-active organometallics, to redox-switch receptors. The significant potential of this special class of ferrocenes is expected to witness further exploration in many fronts.

References

[1] P.L. Pauson, T.J. Kealy, Nature 168 (1951) 1039.
[2] G. Wilkinson, M. Rosenblum, M.C. Whiting, R.B. Woodward, J. Am. Chem. Soc. 74 (1952) 2125.
[3] P.F. Eiland, R. Pepinsky, J. Am. Chem. Soc. 74 (1952) 4971.
[4] E.O. Fischer, W.Z. Pfab, Naturforsch b 7 (1952) 377.
[5] A. Togni, T. Hayashi (Eds.), Ferrocenes: Homogeneous Catalysis, Organic Synthesis, Material Science, VCH, Weinheim, 1995.
[6] T.J. Colacot, Chem. Rev. 103 (2003) 3101.
[7] P. Barbaro, C. Bianchini, G. Giambastiani, S.L. Parisel, Coord. Chem. Rev. 248 (2004) 2131.
[8] N.S. Hosmane, Z. Anorg. Allg. Chem. 631 (2005) 259 (and references therein).
[9] J.L. Serrano (Ed.), Metallomesogens: Synthesis, Properties and Applications, VCH, Weinheim, 1996.
[10] D. Apreutesei, G. Lisa, D. Scutaru, N. Hurduc, J. Optoelectron. Adv. M 8 (2006) 737.
[11] A.E. Kaifer, S. Mendoza, in: J.L. Atwood, J.E.D. Davies, D.D. Macnicol, F. Vögtle (Eds.), Comprehensive Supramolecular Chemistry, vol. 1, Elsevier, New York, 1996, p. 701.
[12] I. Haiduc, F.T. Edelmann, Supramolecular Organometallic Chemistry, Wiley–VCH, Weinheim, 1999, p. 37.
[13] P.L. Boulas, M. Gómez-Kaifer, L. Echegoyen, Angew. Chem. Int. Ed. 37 (1998) 216.
[14] J.H.R. Tucker, S.R. Collinson, Chem. Soc. Rev. 31 (2002) 147.
[15] J. Westwood, S.J. Coles, S.R. Collinson, G. Gasser, S.J. Green, M.B. Hursthouse, M.E. Light, J.H.R. Tucker, Organometallics 23 (2004) 946 (and references therein).
[16] P.D. Beer, Chem. Soc. Rev. 18 (1989) 409.
[17] P.D. Beer, P.A. Gale, G.Z. Chen, Coord. Chem. Rev. 185/186 (1999) 3.
[18] P.D. Beer, P.A. Gale, G.Z. Chen, J. Chem. Soc., Dalton Trans. (1999) 1897.
[19] U.H.F. Bunz, J. Organomet. Chem. 683 (2003) 269.
[20] B. Alonso, J. Losada, Coord. Chem. Rev. 193–195 (1999) 395.
[21] A.S. Abd-El-Aziz, E.K. Todd, Coord. Chem. Rev. 246 (2003) 3.
[22] D.R. Van Staveren, N. Metzler-Nolte, Chem. Rev. 104 (2004) 5931.
[23] S. Top, B. Dauer, J. Vaissermann, G. Jaouen, J. Organomet. Chem. 541 (1997) 355.
[24] J.D. Carr, S.J. Coles, M.B. Hursthouse, M.E. Light, E.L. Munro, J.H.R. Tucker, J. Westwood, Organometallics 19 (2000) 3312.
[25] T.G. Sprigings, C.D. Hall, Organometallics 20 (2001) 2560.
[26] S.-J. Jong, J.-M. Fang, J. Org. Chem. 66 (2001) 3533.
[27] J. Liu, R. Castro, K.A. Abboud, A.E. Kaifer, J. Org. Chem. 65 (2000) 6973.
[28] D. Naskar, S.K. Das, L. Giribabu, B.G. Maiya, S. Roy, Organometallics 19 (2000) 1464.
[29] K. Dhanalakshmi, G. Sundararajan, J. Organomet. Chem. 645 (2002) 27.
[30] S. Barlow, S.R. Marder, Chem. Commun. (2000) 1555.
[31] E. Peris, Coord. Chem. Rev. 248 (2004) 279 (and references therein).
[32] M. Gómez, E. Peris, H. Teruel, I. Arevalo, J. Mata, G. Muller, Polyhedron 23 (2004) 611.

[33] P.D. Beer, C. Blackburn, J.F. McAleer, H. Sikanyika, Inorg. Chem. 29 (1990) 378.
[34] Y.J. Chen, D.-S. Pan, C.-F. Chiu, J.-X. Su, S.J. Lin, K.S. Kwan, Inorg. Chem. 39 (2000) 953.
[35] A. Hradsky, B. Bildstein, N. Schuler, H. Schottenberger, P. Jaitner, K.-H. Ongania, K. Wurst, J.-P. Launay, Organometallics 16 (1997) 392.
[36] K.R.J. Thomas, J.T. Lin, Y.S. Wen, Organometallics 19 (2000) 1008.
[37] J.-G. Rodŕiguez, M. Gayo, I. Fonseca, J. Organomet. Chem. 534 (1997) 35.
[38] B. Bildstein, P. Denifl, K. Wurst, M. André, M. Baumgarten, J. Friedrich, E. Ellmerer-Müller, Organometallics 14 (1995) 4334.
[39] J.A. Mata, E. Peris, Inorg. Chim. Acta 343 (2003) 175.
[40] A. Peruga, J. Mata, D. Sainz, E. Peris, J. Organomet. Chem. 637–639 (2001) 191.
[41] K.-Y. Kay, Y.G. Baek, D.W. Han, S.Y. Yeu, Synthesis (1997) 35.
[42] V. Chandrasekhar, G.T.S. Andavan, S. Nagendran, V. Krishnan, R. Azhakar, R.J. Butcher, Organometallics 22 (2003) 976.
[43] C. Muthiah, K.P. Kumar, C.A. Mani, K.C. Kumara Swamy, J. Org. Chem. 65 (2000) 3733.
[44] J.C. Torres, R.A. Pilli, M.D. Vargas, F.A. Violante, S.J. Garden, A.C. Pinto, Tetrahedron 58 (2002) 4487.
[45] S. Köcher, H. Lang, J. Organomet. Chem. 637–639 (2001) 198.
[46] W.-Y. Wong, G.-L. Lu, K.-F. Ng, K.-H. Choi, Z. Lin, J. Chem. Soc., Dalton Trans. (2001) 3250.
[47] J.T. Lin, J.J. Wu, C.-S. Li, Y.S. Wen, K.-J. Lin, Organometallics 15 (1996) 5028.
[48] W.-Y. Wong, K.-Y. Ho, S.-L. Ho, Z. Lin, J. Organomet. Chem. 683 (2003) 341.
[49] E. Hendrickx, A. Persoons, S. Samson, G.R. Stephenson, J. Organomet. Chem. 542 (1997) 295.
[50] N. Chawdhury, N.J. Long, M.F. Mahon, L. Ooi, P.R. Raithby, S. Rooke, A.J.P. White, D.J. Williams, M. Younus, J. Organomet. Chem. 689 (2004) 840.
[51] Y. Zhu, M.O. Wolf, J. Am. Chem. Soc. 122 (2000) 10121.
[52] E.M. McGale, B.H. Robinson, J. Simpson, Organometallics 22 (2003) 931.
[53] W.-Y. Wong, G.-L. Lu, K.-H. Choi, Y.-H. Guo, J. Organomet. Chem. 690 (2005) 177.
[54] H. Fink, N.J. Long, A.J. Martin, G. Opromolla, A.J.P. White, D.J. Williams, P. Zanello, Organometallics 16 (1997) 2646.
[55] Y. Zhu, O. Clot, M.O. Wolf, G.P.A. Yap, J. Am. Chem. Soc. 120 (1998) 1812.
[56] B. Bildstein, Coord. Chem. Rev. 206/207 (2000) 369.
[57] W. Skibar, H. Kopacka, K. Wurst, C. Salzmann, K.-H. Ongania, F.F. de Biani, P. Zanello, B. Bildstein, Organometallics 23 (2004) 1024.
[58] J.A. Mata, E. Falomir, R. Llusar, E. Peris, J. Organomet. Chem. 616 (2000) 80.
[59] K.R.J. Thomas, J.T. Lin, Y.S. Wen, J. Organomet. Chem. 575 (1999) 301.
[60] W.M. Horspool, R.G. Sutherland, Can. J. Chem. 46 (1968) 3453.
[61] J.A. Mata, S. Uriel, R. Llusar, E. Peris, Organometallics 19 (2000) 3797.
[62] A. Togni, M. Hobi, G. Rihs, G. Rist, A. Albinati, P. Zanello, D. Zech, H. Keller, Organometallics 13 (1994) 1224.
[63] A. Chesney, M.R. Bryce, A.S. Batsanov, J.A.K. Howard, L.M. Goldenberg, Chem. Commun. (1998) 677.
[64] X. You, H. Sun, X. Peng, C. Yue, C. Li, H. Wu, Inorg. Chim. Acta 234 (1995) 139.
[65] W. Liu, Q. Xu, Y. Ma, Y. Liang, N. Dong, D. Guan, J. Organomet. Chem. 625 (2001) 128.
[66] B. W. Ponder, C.W. Barnhill, US Patent 3,739,004 (1973).
[67] D.C. Van Landuyt, US Patent 3,751,441 (1973).
[68] C. Qiu, Y. Zhang, Huaxue Shiji 14 (1992) 104.
[69] A. Kundu, S. Prabhakar, M. Vairamani, S. Roy, Organometallics 16 (1997) 4796.
[70] P. Sinha, S. Roy, Chem. Commun. (2001) 1798.
[71] P. Debroy, S. Roy, J. Organomet. Chem. 675 (2003) 105.
[72] P. Debroy, S. Roy, Indian J. Chem., Sec. A 42 (2003) 2416.
[73] I. Cuadrado, M. Moran, C.M. Casado, B. Alonso, J. Losada, Coord. Chem. Rev. 193–195 (1999) 395.
[74] V. Alain, A. Fort, M. Barzoukas, C.-T. Chen, M. Blanchard-Desce, S.R. Marder, J.W. Perry, Inorg. Chim. Acta 242 (1996) 43.
[75] E. Stankovic, S. Toma, R.V. Boxel, I. Asselberghs, A. Persoons, J. Organomet. Chem. 637–639 (2001) 426.
[76] M.A. Buretea, T.D. Tilley, Organometallics 16 (1997) 1507.
[77] R.W. Heo, J.-S. Park, T.R. Lee, Macromolecules 38 (2005) 2564.
[78] W.G. Jary, A.-K. Mahler, T. Purkathofer, J. Baumgartner, J. Organomet. Chem. 629 (2001) 208 (and references therein).
[79] T. Yasuda, J. Abe, T. Iyoda, T. Kawai, Chem. Lett. (2001) 812.
[80] P. Debroy, D. Naskar, S. Roy, Inorg. Chim. Acta 359 (2006) 1215.
[81] O. Lavastre, J. Plass, P. Bachmann, S. Guesmi, C. Moinet, P.H. Dixneuf, Organometallics 16 (1997) 184.
[82] J.T. Lin, S.-S. Sun, J.J. Wu, L. Lee, K.-J. Lin, Y.F. Huang, Inorg. Chem. 34 (1995) 2323.
[83] L. Carollo, B. Floris, J. Organomet. Chem. 583 (1999) 80.
[84] M.D. Rausch, A. Siegel, L.P. Klemann, J. Org. Chem. 31 (1966) 2703.
[85] A.-C. Ribou, J.-P. Launay, M.L. Sachtleben, H. Li, C.W. Spangler, Inorg. Chem. 35 (1996) 3735.
[86] C. Levanda, K. Bechgaard, D.O. Cowan, J. Org. Chem. 41 (1976) 2700.
[87] R. Frantz, J.-O. Durand, G.F. Lanneau, J. Organomet. Chem. 689 (2004) 1867.
[88] P. Štěpnička, L. Trojan, J. Kubišta, J. Ludvik, J. Organomet. Chem. 637–639 (2001) 291.
[89] N.J. Long, Metallocenes—An Introduction to Sandwich Complexes, Blackwell Science, Oxford, 1998 (Chapter 3).
[90] R.W. Heo, F.B. Somoza, T.R. Lee, J. Am. Chem. Soc. 120 (1998) 1621.
[91] M.L.H. Green, S.R. Marder, M.E. Thompson, J.A. Bandy, D. Bloor, P.V. Kolinsky, R.J. Jones, Nature 330 (1987) 360.
[92] S.D. Bella, Chem. Soc. Rev. 30 (2001) 355.
[93] J. Heck, S. Dabek, T. Meyer-Friedrichsen, H. Wong, Coord. Chem. Rev. 190–192 (1999) 1217 (and references therein).
[94] J.C. Calabrese, L.-T. Cheng, J.C. Green, S.R. Marder, W. Tam, J. Am. Chem. Soc. 113 (1991) 7227.
[95] M. Kurihara, H. Sano, M. Murata, H. Nishihara, Inorg. Chem. 40 (2001) 4.